"GREEN HYDROGEN" VIA PHOTOELECTROCATALYSIS

V.A. Majidzade[1*], S.F. Jafarova[1], S.P. Javadova[1], A.N. Azizova[2], F.B. Aliyeva[1], S.N. Baylarli-Sadiyeva[3], N.I. Shikhaliyev[4]

[1]Institute of Catalysis and Inorganic Chemistry named after M. Nagiyev MSE of Azerbaijan, AZ 1143, H. Javid ave.113, Baku, Azerbaijan
[2]Azerbaijan Medical University, Scientific Research Centre, Baku, Azerbaijan
[3]Mingachevir State University
[4]Azerbaijan Technical University MSE of Azerbaijan
[*]e-mail: vuska.macidzade.80@gmail.com

Received 14.05.2025
Accepted 06.07.2025

Abstract: *The growing global demand for clean and sustainable energy sources has intensified interest in green hydrogen as a carbon-free fuel. Among the various pathways for green hydrogen generation, photoelectrocatalysis (PEC) has gained significant attention due to its unique ability to directly convert solar energy into chemical energy through water splitting. This review provides a comprehensive overview of recent progress in PEC-driven hydrogen production.*
Key classes of photoelectrocatalysts—including metal oxides, chalcogenides, perovskites, and emerging two-dimensional materials—are analyzed with respect to their optical absorption, band alignment, stability, and catalytic activity. Challenges such as limited light absorption, rapid charge recombination, corrosion, and scalability constraints are critically discussed. Finally, future directions for achieving commercially viable PEC hydrogen generation are outlined, earth-abundant catalysts and systems engineering approaches. Overall, this review underscores the potential of photoelectrocatalysis as a promising pathway for large-scale green hydrogen production powered by sunlight.
Keyword: *photocatalysis, Hydrogen energy, Solar energy, photocathode, photoanode, metal chalcogenide.*
DOI: 10.65382/2221-8688-2026-2-149-182

Introduction

Solar photocatalysis and photoelectrocatalysis have emerged as highly promising approaches for achieving clean, cost-effective, and sustainable renewable energy generation, as well as enabling efficient removal of pollutants [1].

Photoelectrocatalysis (PEC) is a new technology designed to overcome the limitations of traditional photocatalysis. It involves immobilizing a photocatalyst on a conductive substrate, which simultaneously functions as an electrode [2, 3, 4]. It is a powerful method obtained from the combination of heterogeneous photocatalysis and an electrochemical process. The process involves utilizing a semiconductor that is exposed to light with energy equal to or greater than its band gap energy while simultaneously applying a gradient potential across the semiconductor [4]. The basic concept is that when a semiconductor surface is exposed to light ($h\nu \geq E_g$), electron/hole pairs (e^-/h^+) are generated by promoting an electron from the valence band (lower energy level) to the conduction band (higher energy level). Electrons are guided toward the counter electrode under positive potential in n-type materials to reduce the recombination of electron-hole pairs, which is significant due to their short lifetimes. When immersed in an electrolyte, adsorbed water molecules and/or hydroxyl ions react with holes in the valence band to form hydroxyl radicals (●OH), which are a powerful oxidizing agent (+2.80 V) [5-8]. Compared to photocatalysis, the FEC process shows higher efficiency and produces a larger number of holes [2]. The immobilization of the photoelectrocatalyst is a significant advantage of the FEC process.

As a rule, photocatalytic processes mainly include three main stages: 1) generation of electron-hole pairs by absorption of photons with

higher energy than the forbidden zone (E_g) of photocatalysts (photoelectrodes), 2) separation of charges and their migration to the surface of the photocatalyst, and 3) reduction/oxidation reaction occurring on the surface of the photocatalysts [9-11].

Currently, the transition to solar energy appears highly promising, as solar power generation does not pollute the environment or disrupt the Earth's overall energy balance. There are several possible applications of solar energy, including serving as a heat source for building heating [12]; heating and desalination of water [13, 14]; generating electricity with heat engines [15, 16]; and direct conversion to electricity using semiconductor converters [17, 18]. The sun's periodic activity necessitates storing it in power plants to provide electricity during periods without sunlight. One of the most efficient methods of energy storage is to produce hydrogen, which can later be used in fuel cells to generate electricity. From this perspective, one should consider either the photoelectric conversion of light energy into electrical energy followed by water electrolysis with sufficiently high efficiency, such as high-temperature or solid-polymer electrolysis, or photoelectrochemical processes, in which hydrogen and oxygen are formed on photosensitive electrodes made of n- and p-type semiconductors due to charge carriers generated by light and separated by the field of the space charge region.

A crucial challenge for photoelectrochemical water splitting is the development of corrosion-resistant semiconductor electrode materials with a band gap that matches the energy required for water decomposition. Although the process of water photoelectrolysis has been studied by many researchers, systems that meet the requirements have not yet been found. There are semiconductor materials that are acceptable at least in terms of certain individual characteristics, such as stability, band gap width (E_g), flat band potential (φ_{fb}), etc. [19].

For effective water photoelectrolysis, it is essential to eliminate all side effects, especially photocorrosion of the semiconductor electrode. This requires that the condition $\varphi^\circ_{H_2O/O_2} < \varphi^\circ_{dec,p}$ (for an n-type semiconductor) or $\varphi^\circ_{H_2/H_2O} < \varphi^\circ_{dec,n}$ (for a p-type semiconductor) be satisfied [19].

Therefore, the following conditions must be satisfied for water photoelectrolysis to proceed effectively [19]:

1. The band gap width must exceed the difference in electrochemical potentials between the hydrogen and oxygen reactions in water (1.23 eV); in other words, $Eg > F_{H2/H2O} - F_{H2O/O2}$;
2. The energy of the light quanta must be greater than the band gap, $h\omega > Eg$;
3. The flat band potential of an n-type semiconductor should be more negative than the hydrogen electrode potential, while that of a p-type semiconductor should be more positive than the oxygen electrode potential.

Currently, various photoelectrodes are used for photoelectrocatalysis. Selecting the appropriate photoanode and/or photocathode material is the most critical aspect of this process. An ideal photoanode and/or photocathode for photoelectrochemical water splitting requires semiconductor materials with the following characteristics [20]:

1) **Suitable band gap energy and energy band positions**. Natural sunlight consists of 5% UV (300–400 nm), 43% visible (400–700 nm), and 52% infrared radiation (700–2500 nm) [20]. Therefore, to improve efficiency, the semiconductor must significantly absorb light in the visible region, a property determined by its band gap. Since the proton reduction potential is 0 V vs NHE and the O_2/H_2O potential is 1.23 V NHE (at pH = 0), the theoretical minimum band gap for water splitting requires incident photons with at least 1.23 eV of energy, which corresponds to a light wavelength of approximately 1100 nm. However, taking into account thermodynamic energy losses (0.3–0.4 eV) occurring during charge carrier transport and the overpotential required for acceptable surface reaction kinetics (0.4–0.6 eV), a minimum band gap of ~1.8 eV is required, which corresponds to light absorption at approximately 700 nm. The upper limit of the band gap energy is 3.2 eV due to the rapid decrease in sunlight intensity below 390 nm, consistent with the solar spectrum. Thus, for a single semiconductor photoelectrode, band gap energy between 1.9 eV and 3.2 eV is desirable to achieve significant photovoltage [20].

2) **Efficient separation and transport of charge carriers in a semiconductor**. Efficient separation and transport of charge carriers in a semiconductor. Rapid charge recombination is a primary cause of low solar-to-hydrogen conversion efficiency; therefore, a strategy is required to promote the efficient separation and transport of charge carriers, which depend on both the intrinsic properties (hole and electron mobility) and extrinsic properties (crystallinity, nanostructure) of the material [11].
3) **Strong catalytic activity and stability.** Sufficiently fast surface reaction kinetics can prevent surface charge accumulation, which would otherwise lead to electron-hole recombination. Photocorrosion poses a significant challenge for many semiconductor candidates used in water splitting, especially metal sulfides, and occurs when photogenerated holes or electrons, instead of driving water oxidation or reduction, react with and degrade the photocatalyst itself. These photocorrosion reactions are influenced by the relative positions of the semiconductor band edges and their corresponding decomposition potentials. Anodic photocorrosion may occur if the anodic decomposition potential (E_{pd}) exceeds the valence band potential of the semiconductor. Conversely, cathodic photocorrosion may occur if the cathodic decomposition potential ($_{End}$) is lower than the conduction band potential of the semiconductor. Metal oxides such as $BiVO_4$ and ZnO, as well as metal sulfides like MoS_2 and CdS, can be susceptible to anodic photocorrosion depending on the pH of the electrolyte, since the actual decomposition potential values are pH-dependent. However, conventional photoanode materials such as TiO_2 and Fe_2O_3, despite having water decomposition potentials above their valence band potentials, are thermodynamically stable because their decomposition reactions proceed at very slow kinetic rates [11, 19].

Furthermore, for practical applications, photoelectrode materials should be low-cost and composed of elements that are abundant on Earth. This is essential to support the case for economically scalable solar-to-fuel devices [11].

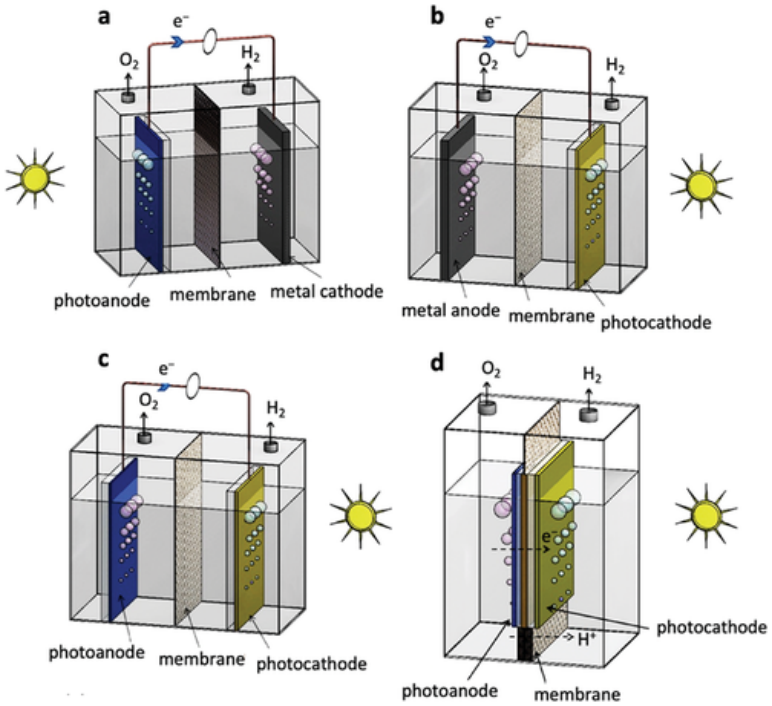

Fig. 1. Schematic representation of some photoelectrochemical devices: a) photoanode with metal cathode, b) photocathode with metal anode, c) wire tandem photoelectrochemical cell with photoanode and photocathode, and d) wireless tandem photoelectrochemical device [22, 23]

In addition, developing a device that is both efficient and stable for converting solar energy into hydrogen remains a significant challenge [11, 20]. Although recent reports have shown

water splitting devices achieving 30% efficiency by coupling a photovoltaic cell with an electrolyzer [21], current research is focused on developing direct, low-cost, and highly water splitting through photoelectrochemical cells.

This is due to two main driving forces. First, a low voltage is required to control the photoelectrochemical decomposition of water, which promises a higher efficiency of converting solar energy into hydrogen, despite the fact that several photovoltaic cells are usually used in series to achieve the minimum potential (3.0 V, required by the electrolyzer in the indirect path). Secondly, photoelectrochemical decomposition of water requires a much simpler and more compact design with fewer components (wires, electrodes, reactor, etc.) [11].

The primary components of photoelectrochemical devices for water splitting are semiconductor light-absorbing photoelectrodes, an electrolyte, and a separation membrane [11].

Typical photoelectrochemical systems may feature a single photoelectrode (photocathode or photoanode) paired with a counterelectrode, or a tandem structure incorporating both a photoanode and a photocathode to enhance photopotential and light absorption (Fig. 1) [22-25].

The water decomposition reaction is a process that requires a minimum Gibbs free energy of 237 kJ·mol^{-1} [10]. As shown in Fig. 2, there are three main physical and chemical processes involved in the full reaction of the photoelectrochemical decomposition of water.

The first step of the process involves the absorption of light from a calibrated source—commonly simulating solar irradiation (e.g., 100 mW·cm^{-2})—by a semiconductor photoelectrode. In typical photoelectrochemical systems, an n-type semiconductor functions as the photoanode, whereas a p-type semiconductor serves as the photocathode. Upon absorption of photons with energies exceeding the semiconductor band gap (Eg), electron–hole pairs are generated: electrons are promoted to the conduction band, while holes remain in the valence band.

For water oxidation to proceed, the valence band edge of the semiconductor must be positioned at a potential more positive than the O_2/H_2O redox potential (1.23 V vs. the normal hydrogen electrode, NHE, at pH = 0). Conversely, for water reduction to occur, the conduction band edge must be located at a potential more negative than the H^+/H_2 redox potential (0 V vs. NHE at pH = 0).

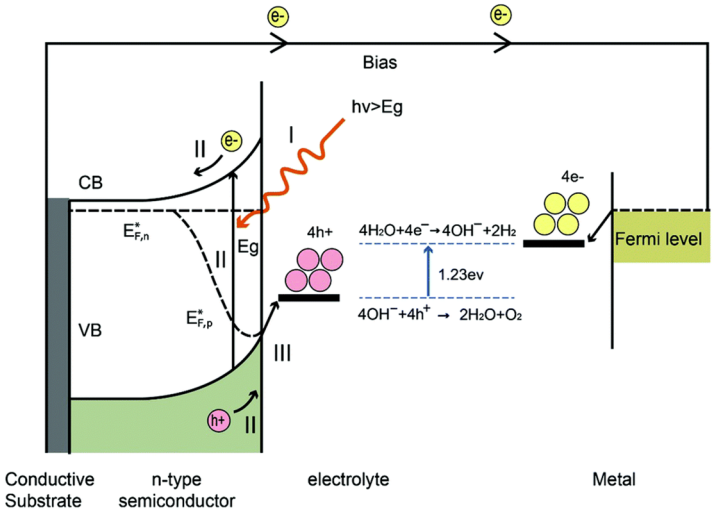

Fig. 2. Schematic of a simple photoelectrochemical cell based on an n-type semiconductor photoanode electrically connected to a metal counter electrode under external influence, maintained under alkaline conditions. At the photoanode, the reaction $4OH^- + 4H^+ \rightarrow 2H_2O + O_2$ occurs and because of the conduction band position is positive, a voltage is required to accelerate the reduction of water effectively. The main processes include: (I) light absorption; (II) carrier separation and transport; and (III) surface redox reactions [11]

Note that additional voltage is required to compensate for energy losses associated with the movement of photoholes through the space charge region, as well as the transfer of electrons through the external circuit to the counter electrode (such as platinum). The second process is the separation and transport of photogenerated electron-hole pairs. During these steps, charge carriers may recombine either within the bulk of the material or at its surface, and therefore, both efficient charge separation and high charge carrier mobility are desirable. The last process is the surface reaction, where oxidation-reduction reactions occur to break down water. Both an appropriate charge carrier potential and favorable kinetics of reaction are essential for efficient water splitting [11].

Currently, great attention is being paid to increasing both the efficiency of solar-to-hydrogen conversion and its long-term operational stability. The highest solar-to-hydrogen conversion for without applying external voltage water splitting is 19.3% and is achieved with this multi-junction monolithic III–V semiconductor photoelectrochemical device [21, 22]. Despite this significant milestone, the high cost of III–V semiconductor materials has limited their commercial viability. In contrast, binary metal oxides (Fe_2O_3, WO_3, Cu_2O), chalcogenides (CdS, MoS_2, WSe_2), oxynitrides (TaON, $LaTiO_2N$), multicomponent compounds ($BiVO_4$, Fe_2TiO_5, $NiMoO_4$), and carbon-based materials have been extensively studied as inexpensive, efficient, and reliable photoelectrocatalysts [26-28].

The primary challenges to address involve both system configurations and material properties. Typical problems with the latter include limited light absorption, high carrier recombination rates, slow charge transport at the semiconductor-liquid interface, low photocurrent density, limited efficiency, poor stability, and photocorrosion. All these aspects are serious obstacles to the development of effective devices [29, 30]. In this context, material selection is a game-changer, as it considers not only technical limitations but also geopolitical availability and fluctuating market prices. Strategies for increasing activity and stability are based on adapting the semiconductor structure through doping, surface modification with defects or functional groups, nanostructuring, and heterojunction formation [31-33].

Photoelectrodes for efficient photoelectrocatalytic hydrogen production can be obtained by various methods [34]: one-stage hydrothermal synthesis [35-37], the solvothermal method [38], sulfidation and selenization [39], the free intercalation method [40], the sequential ion layer adsorption and reaction (SILAR) method [41], the electrodeposition method [42-43], the photoreduction method [44], chemical vapor deposition (CVD) [45], the sequential surface modification method [46], and microwave-assisted synthesis [47-50].

Photoelectrodes. To date, dozens of semiconductor materials have been investigated as photoelectrodes for photoelectrochemical water splitting. The majority of these materials are *n*-type semiconductors, while only a limited number exhibit *p*-type conductivity. However, none of the studied materials simultaneously satisfy the full set of requirements necessary for efficient solar-driven water photoelectrolysis. In this review, attention is focused on semiconductor materials that have demonstrated at least partial suitability as photoelectrodes. Among the key electrode requirements, the development of corrosion-resistant semiconductor anodes with a band gap appropriately matched to the thermodynamic energy required for water decomposition is of particular importance for photoelectrochemical applications. Although photoelectrochemical water splitting has been intensively studied in recent years, no material system fully meeting all performance criteria has yet been identified and research in this area remains ongoing. Nevertheless, several semiconductor materials exhibit acceptable photoelectrochemical characteristics in certain aspects, such as chemical stability, band gap width (E_g), and flat-band potential (φ_{n3}), making them promising candidates for further investigation [19].

For this reason, at present, semiconductor materials capable of converting solar energy into chemical energy are divided into two groups: semiconductors that are sufficiently stable in aqueous electrolyte solutions but have a maximum photosensitivity not in the visible but in the ultraviolet region of the spectrum (TiO_2, WO_3, SnO_2, etc.); and semiconductors that have a maximum photosensitivity in the visible region of the spectrum but a minimum stability in

aqueous electrolyte solutions (CdS, CdSe, CdTe, GaAs, GaP, InP, etc.) [19].

As is known, photoanodes and photocathodes have different applications.

A photoanode is an electrode that participates in photoelectrochemical processes, where it acts as an anode (positive electrode) and is activated by light. **A photoanode** is an anode on the surface of which, under the influence of light, oxidation reactions occur, usually involving water or other substances, resulting in the release of electrons. The photoanodes are made of semiconductor materials. Under the influence of light, electron-hole pairs are formed in the semiconductor; the electrons leave through the external circuit, and the holes remain and participate in the oxidation of water or other substances on the surface of the photoanode. In a photocatalytic water splitting setup, light falls on a photoanode, water on the surface of the photoanode is oxidized to form oxygen, and electrons flow through a circuit to the cathode, where protons are converted to hydrogen.

Photoelectrodes based on **TiO_2** for water decomposition have been intensively studied since 1972 due to many favorable properties [11]. The first is that they are composed of non-toxic elements common in the earth and are also photochemically stable in both highly acidic and highly alkaline conditions [51, 52]. TiO_2 is a corrosion-resistant oxide semiconductor that has various crystalline modifications – usually rutile, less commonly anatase and brookite.

However, due to its wide band gap (3.2 eV for anatase and 3.0 eV for the rutile phase), only about 5% of the solar spectrum (primarily UV radiation) can be absorbed. This results in a very low maximum theoretical solar-to-hydrogen energy conversion efficiency (η = 1.3% for anatase and 2.2% for rutile TiO_2) [11]. Over the past decade, many attempts have been made to dope TiO_2 with anions or cations to extend its working range into the visible region, thereby improving overall absorption while maintaining its high stability and low cost [3, 53]. The valence band of TiO_2 can be modified by introducing non-metallic species such as carbon or nitrogen to form states in the middle of the band gap [54], and the conduction band can be modified by forming donor states below it through doping with 3d transition metal ions. Since there is no fundamental change in the band gap for these materials in most examples, no significant enhancement of water decomposition activity in the visible range was observed. Although doping can broaden light absorption into the visible range, the optical absorption remains moderate above $\lambda > 450$ nm. Recently, the authors of [55] developed a new strategy to synthesize a disordered TiO_2 nanophase by incorporating dopants through the hydrogenation of TiO_2 nanocrystals. The prepared hydrogenated TiO_2 is black in color, corresponding to a band gap energy of 1.0 eV, compared to the typical 3.30 eV for pure TiO_2, and thus promises much higher solar-to-fuel conversion efficiency [56]. As shown by studies using electron spectroscopy for chemical analysis, Ti^{3+} ions in the TiO_2 lattice, which act as electron donors, are re-oxidized to Ti^{4+} during the oxygen photoevolution process, and the oxygen vacancies are filled, and the titanium oxide becomes stoichiometric. In addition, TiO_2 titanium-containing materials are also used as photoanode materials for converting solar energy into hydrogen.

Fe_2O_3 (hematite) is a promising photoanode material owing to its good chemical stability, low toxicity, low cost, and high natural abundance. In addition, it has a band gap value of 1.9 to 2.32 eV, which allows it to absorb visible light, which corresponds to the maximum theoretical efficiency of converting solar energy into hydrogen [57]. Hematite also has some disadvantages:

- short lifetime of charge carriers of the order of picoseconds due to rapid recombination of charge carriers in the volume;
- relatively low absorption coefficient (about 10^3 cm^{-1}), requiring a film thickness of at least 400–500 nm for optimal light absorption;
- slow mobility of minority charge carriers (holes) (approximately 0.2 $cm^2 \cdot V^{-1} \cdot s^{-1}$), which results in a very short hole diffusion length of 2–4 nm;
- poor water oxidation kinetics, resulting in high recombination rates on the surface due to hole accumulation [58].

To overcome these limitations, several strategies have been applied to improve the activity of hematite-based photoelectrodes [59]. Firstly, it has been shown that high concentration doping with various elements such as Si, Ti and P improves the electron conductivity in hematite.

In this regard, Si-doped hematite nanocrystalline films can exhibit high photoelectrochemical performance with a photocurrent density of at least 2.7 mA cm^{-2} at 1.23 V compared to a normal hydrogen electrode under irradiation by a single AM 1.5G sun [59]. In addition, introducing thin metal oxide sublayers or overlayers on α-Fe_2O_3 significantly improves its photoelectrochemical activity by enhancing surface-state passivation and increasing the concentration and mobility of charge carriers [60, 61]. However, recent studies report a benchmark photocurrent of 4.68 mA cm^{-2} at 1.23 V (vs. the normal hydrogen electrode) and a solar-to-hydrogen conversion efficiency of about 0.55% for hematite. These results were achieved using a vertically grown hematite nanosheet film modified with Ag nanoparticles and a Co–P_i cocatalyst. Despite this progress, much more work is needed to improve the solar-to-hydrogen conversion performance, considering that the material's limitations are fairly well understood [60, 62-63].

$SrTiO_3$ is the only metal oxide that can decompose water without assistance in a two-electrode system [64]. The band gap of this titanate is 3.2 eV, and because of this large band gap, its photo-conversion efficiency is below 1%. To enhance the efficiency, the authors investigated the spectral sensitization of $SrTiO_3$ photoanodes using several ruthenium (II) complexes [65-67].

$BaTiO_3$ is a common perovskite oxide with a band gap energy of about 3.2 eV and has the ability to decompose water into hydrogen and oxygen to its appropriate position in the conduction and valence bands [68, 69]. Electrons with high reducing power in the conduction band and holes with sufficient oxidizing power in the valence band are usually required for efficient photocatalytic reactions [70, 71]. Due to its unique physical and chemical properties, many studies have been conducted to overcome the limitations that hinder the improvement of photocatalytic efficiency [69, 72-73]. Among the factors influencing the photocatalytic activity of $BaTiO_3$, the relatively high recombination rate of photoexcited electrons and holes is the primary cause of the low photocatalytic efficiency [74, 75]. Thus, some effective approaches have been explored to promote the separation and migration of photogenerated carriers, such as noble metal loading, ion doping, heterogeneous structure, and size and morphology control. Thus, some effective approaches have been explored to promote the separation and migration of photogenerated carriers, such as noble metal loading, ion doping, heterogeneous structure, and size and morphology control [68, 70, 76-79].

Currently, photoanodes based on III–V compounds are the most promising [59, 71, 80-81].

$BiVO_4$ is an n-type semiconductor composed of relatively common elements on Earth [11]. It has a direct band gap of 2.4 eV with a conduction band position close to 0 V compared to NHE (pH = 0) and a valence band position around +2.4 eV compared to NHE (pH = 0) described in [82]. Following this discovery, $BiVO_4$ was also used as a photoanode for photoelectrochemical water decomposition, a progress that was reviewed in detail by other researchers [83]. The theoretical maximum photocurrent and solar-to-hydrogen conversion efficiency of $BiVO_4$ are 7.4 mA cm^{-2} at 1.23 V compared to RHE and 9.1%, respectively. The efficiency of $BiVO_4$ is limited by several factors. Rapid charge carrier recombination remains a major challenge due to the short electron diffusion length (only about 10 nm). However, this diffusion length can be significantly increased to approximately 300 nm by doping with Mo or W [84]. Other authors [85] introduced gradient tungsten doping, starting with 1% W at the $BiVO_4$ electrolyte interface, to enhance charge carrier separation efficiency. Moreover, the carrier separation efficiency increases to about 60% at 1.23 V vs. RHE, compared to about 38% for uniformly doped $BiVO_4$. This improvement is attributed to the expansion of the band bending region throughout the entire thickness of the $BiVO_4$ photoanode, thereby enhancing carrier separation. In detail, when W-doped and undoped $BiVO_4$ are brought into contact, the Fermi energy levels are balanced by electron transfer from the W-doped portion to the undoped portion of the material. A depletion layer then forms at the interface between the W-doped and undoped $BiVO_4$ [85].

Gallium arsenide (GaAs) is an important semiconductor with a direct band gap of 1.42 eV that is commonly used to produce devices such as infrared emitting diodes, laser diodes, microwave integrated circuits, and photovoltaic

cells [57, 86-90]. GaAs has a high electron mobility that exceeds that of silicon, which makes it suitable for high-speed applications such as microwave devices, high-speed transistors, and integrated circuits (ICs).

The authors in [91] reported that applying a TiO_2 film onto GaAs effectively suppresses photocorrosion while preserving the system's sensitivity to visible light. In addition, it was found that the GaAs-based photocathode achieves higher quantum efficiency and a longer lifetime under 633 nm monochromatic light illuminations, an advantage that can hardly be obtained by simply adjusting the intensity of white light [92, 93].

GaAs has been widely used in recent years as a high average current and polarized electron source in several accelerators and light sources. Their applications have also been found in photomultiplier tubes, high-performance image intensifiers, low-energy electron microscopes (LEEMs), and spin low-energy electron microscopy (SPLEEMs) [94-98]. GaAs photocathodes also offer a number of advantages over other cathodes, including high spin polarization in strained layer structures and very low heat dissipation under certain conditions [99-106]. The main limitation of GaAs photocathodes lies in their short operational lifetime. Their quantum efficiency degrades relatively quickly even under a high vacuum (UHV) system with a pressure of 10^{-10} mbar, even if they are not operated under high voltage and/or powerful illumination [96, 107-109]. The dark lifetime of the quantum efficiency, defined as the time for the quantum efficiency to decay to 1/e of its initial value without electron emission or high voltage applied to the cathode, ranges from several tens to several hundred hours in the best cases, as reported in multiple studies [107, 109-112]. The predominant mechanism behind for this degradation is contamination of the cathode surface by residual gases within the vacuum system [96, 108, 109, 113-116]. To eliminate this problem, a clear understanding of the influence of different gas types on the quantum efficiency of photocathodes is required.

Gallium phosphide (GaP) is a III-V binary semiconductor with a direct band gap of 2.26 eV and therefore absorbs a significant portion of the energy from sunlight [117-119]. GaP is useful in certain optoelectronic applications. It is commonly used in red, orange, and green light-emitting diodes (LEDs). One of GaP's notable advantages is its high thermal conductivity, which allows for better heat dissipation in electronic devices. Although it does not exhibit the same level of efficiency as materials like GaAs in high-frequency applications, GaP is used as a substrate material for other III-V semiconductors such as GaAs and InP to form heterostructure devices. It is also used in photonic integrated circuits and is sometimes used in combination with other semiconductors to develop desired electronic or optical properties. As is known, for the photodecomposition of water in the absence of an external voltage, it is necessary that the potential of the flat zones of the photocathode material be more positive than the potential of the oxygen electrode. Unfortunately, in the case of gallium phosphide, this condition is not met. Therefore, to carry out photoelectrolysis of water, a significant voltage from an external source must be applied to a cell with a GaP photocathode and a platinum anode. This significantly reduces the energy conversion efficiency. Also, the stability of the GaP photocathode under long-term operation conditions proved satisfactory. There is no visible damage to the electrode observed, and gallium does not dissolve in significant amounts. However, the photocurrent gradually decreases over time. In addition to water photodecomposition, the GaP cathode has also been proposed for use in other photoelectrochemical reactions [19].

Cadmium chalcogenides. Theoretically, photocatalytic evolution of H_2 and O_2 upon visible light irradiation can be achieved on pure CdS due to its relatively narrow band gap of 2.4 eV and favorable conduction band-edge positions of -0.7 V and valence band position of +1.7 V relative to NHE (pH = 0) [11]. Although the material exhibits a long charge carrier diffusion length in the micrometer range, its poor water oxidation kinetics lead to accumulation of photogenerated holes on the surface, resulting in severe anodic photocorrosion [120-122]. To mitigate this issue, hole scavengers such as S^{2-} and SO_3^{2-} are typically employed when using CdS for photocatalytic water reduction. Similar to CdS, II–VI semiconductors (e.g., CdS, CdTe, CdSe, and ZnTe) also require stabilization or protection strategies when used as photoanodes

for photoelectrochemical water splitting [123-132]. Surface passivation layers have been widely used to reduce charge recombination at surface states, increase reaction kinetics, and protect the semiconductor from chemical corrosion [133]. CdS photoanodes modified with TiO_2 nanoparticles have also been demonstrated to enable long-term hydrogen production, and CdS photoanodes can also be modified with Nb based nanooxides for efficient and stable photoelectrochemical water splitting [134-136]. Recently, TiO_2/CdS/Co–Pi heterojunction exhibited a photocurrent of approximately 1 $mA \cdot cm^{-2}$ at 1.23 in relatively RHE and showed reasonable stability during 2 h of irradiation, due to photoelectron injection into TiO_2 from CdS and hole transfer to Co–Pi for water oxidation, which mitigated the photocorrosion process to some extent [137]. However, much more work needs to be done to improve the performance and stability of CdS-based photoelectrodes.

Along with CdS used as a photoanode, CdTe was also demonstrated to be protected by a 140 nm-thick amorphous TiO_2 layer (deposited by atomic layer deposition [ALD]), together with a thin top layer of the oxygen evolution electrocatalyst NiO, which exhibited stable photocurrents for four days [138-145]. Among cadmium chalcogenides, CdSe is also a valuable material for photoelectrochemical water decomposition due to its ability to absorb visible light and control the hydrogen evolution reaction. However, its performance can be further improved by combining it in combination with other materials to form heterostructures that improve charge separation, charge transport, and photostability, ultimately leading to higher solar-to-hydrogen conversion efficiency [146-153].

The photocathode is one of the main elements of electron-optical converters [154]. Its function is to emit electrons into a vacuum under the influence of optical radiation, thereby converting an optical image into an electronic one. Its primary parameter is sensitivity, which is determined by the ratio of the photocurrent to the luminous flux that generated it. The photocathode responds to both the intensity and frequency of the luminous flux, so its sensitivity is categorized into integral and spectral [154].

Cu_2O has a direct band gap of about 2 eV, and its conduction band position (approximately -1.1 eV compared to NHE) is suitable for the release of hydrogen from water under the influence of light. [11]. The attractiveness of using Cu_2O lies in its abundance, scalability, low toxicity, and high theoretical photocurrent of about 15 mA cm^{-2}, as well as a potential solar-to-hydrogen conversion efficiency of 18% under 1.5G AM light illumination [155]. However, one of the main drawbacks of Cu_2O is its relatively moderate photocurrent due to the rapid recombination of electrons and holes. An even more serious drawback is its very poor stability, since the redox potentials for the reduction and oxidation of copper oxide lie within the band gap [156, 157]. Several strategies have been used to address these issues, such as: (1) combination with a more positive conduction band n-type semiconductor forms a p–n junction that promotes the rapid transfer of photoelectrons from Cu_2O to the n-type semiconductor, improving not only efficiency but also stability; (2) application of a thin protective layer consisting of, for example, carbon or metal oxide [158-162]. For a stable Cu_2O-based photoelectrochemical electrode, the p–n junction must be continuous and uniform, the protective layer must be conformal and free of pinholes, and the cocatalyst must be strongly and uniformly deposited on the electrode surface [163-164].

Currently, binary and ternary chalcogenide materials are also used as photoelectrodes.

To function effectively, semiconductor photocatalysts require an adequate band gap energy. The band gap, which is defined as the energy difference between a material's valence and conduction bands, plays a crucial role in determining its photocatalytic activity [165]. Although the ideal band gap for efficient H_2 extraction is typically between 1.0 and 2.0 eV, some materials with band gaps greater than 2.0 eV can still perform exceptionally well. This is due to factors such as favorable environmental conditions, enhanced charge separation capabilities, synergistic effects in composite systems, intrinsic catalytic activity, and energy level tuning through doping or surface modification. These materials are able to promote water splitting despite their larger band gaps, highlighting the complex interplay between electrical and catalytic properties in H_2 production. For optimal efficiency, a band gap of about 2 eV is ideal. This energy range allows for the absorption of visible light photons, which

make up a significant portion of the solar spectrum. As a result, it facilitates the excitation of electrons from the valence band to the conduction band under the influence of light [165]. The crystallinity and morphology of photocatalysts influence the rate of H_2 production. A larger surface area results in a greater number of reactive sites, which generates more H_2 [165]. One of the advantages of nanoscale photocatalysts is that their photoinduced charge carriers can more quickly reach photocatalytic surface reaction sites, reducing the rate of recombination. The morphology and structure of photocatalysts depend significantly on the synthesis methods used; changes in temperature, surfactant concentration, and pH can directly affect the size, shape, and structure of the crystals. A review of the literature suggests that most photocatalytic reactions occur on the surface of a photocatalyst. Exposure to specific crystal surfaces, known as the surface effect, can significantly enhance photocatalyst activity. Consequently, the synthesis of photocatalysts with precise morphology and structure has become a key area of research in photocatalysis [166-187].

A study of the effect of temperature revealed that reaction temperature has no thermodynamic impact on photocatalytic activity, as it does not promote the creation of charge carriers. However, increasing the system's operating temperature can enhance product desorption from the photocatalyst surface, which increases photocatalytic activity and improves the reaction rate. The effect of temperature on photocatalytic activity depends on the behavior of the catalyst, which changes when the catalyst is replaced. Lowering the temperature results in low H_2 formation due to slow desorption of the product compared to adsorption of the reactant on the catalytic surface. The high operating temperatures of the system enhance the transfer of charge carriers from valence bands to higher energy states, making the photocatalytic process more efficient against charge carrier recombination and producing more H_2 [188].

The effect of pH on water decomposition varies depending on the chemical system being studied. In water splitting systems, photocatalysts typically operate at a normal pH of 6.7–6.9. The stoichiometric decomposition of pure water balances the concentrations of H^+ and OH^- created, so there is no noticeable difference in the pH of the water before and after the reaction [165].

Metal chalcogenides are known to have better photocatalytic activity compared to oxides [189-192]. However, the main drawback of metal chalcogenides is their poor compositional stability, where they often undergo a photocorrosion process, which destroys the chalcogenides, thereby ultimately reducing the overall photocatalytic efficiency as well as the stability of the catalysts. Compositional instability is essentially an intrinsic characteristic of metal chalcogenides that must be overcome to exploit their inherent potential properties for any given application.

Metal sulfides are considered promising semiconductors due to their efficient light sensitivity. Their valence band, typically formed by sulfur 3p orbitals, exhibits a narrower and more negative range compared to metal oxides, offering unique advantages for photocatalytic applications [194, 195]. Metal sulfides have attracted considerable attention as semiconductor photocatalysts for hydrogen production due to their high photocatalytic activity, abundant active sites, and favorable band structures. Their narrow band gaps allow them to absorb a significant portion of the light spectrum, making them highly efficient for solar power applications [196].

The elements that contribute to the creation of photocatalysts based on metal sulfides are shown in Fig. 3(a) [165, 191]. Fig. 3(b) provides further illustrations of the band structures of several metal sulfides [165, 193]. For photocatalytic production of H_2, various metal sulfides are used as photocatalysts, such as SnS_2 [197-198, 166], CdS [168-169, 199], MoS_2 [169-172, 200], NiS_2 [173-175, 201], WS_2 [176-178], PbS [179], In_2S_3 [180], CuS [181], ZnS [182-187], FeS [202, 203], etc.

Molybdenum disulfide (MoS_2) is a common transition metal dichalcogenide (TMD) known for its unique electronic and optical properties, making it highly efficient in generating hydrogen via photoelectrocatalysis [169-172, 200, 204]. However, pure MoS_2 is often limited in its photoelectrocatalytic performance due to its poor conductivity and limited light absorption capacity [205]. To address these limitations and increase hydrogen

production, the researchers explored a heteroatom doping strategy, which involves introducing different atoms into the catalyst to modulate its conductivity and electronic structure [206].

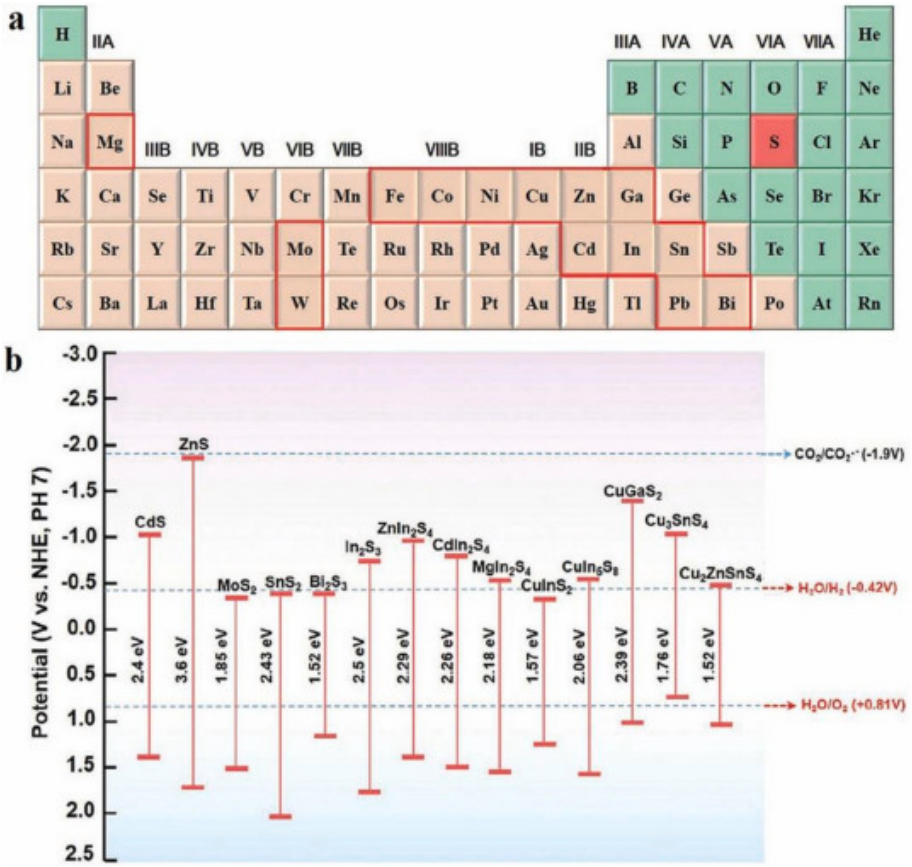

Fig. 3. Image of elements used in the formation of photocatalysts based on metal sulfides (a) and the band gap width of numerous metal sulfides (b) [165, 193].

Multicomponent metal chalcogenides possess desirable characteristics such as narrow band gaps, stability, low toxicity, high photoconductivity, and strong sensitivity to visible light [207]. Initially, these multicomponent metal chalcogenides were mainly used in applications such as photovoltaic and photochemical devices, solar cells, LEDs, and nonlinear optical materials. However, due to their exceptional properties, multicomponent chalcogenides have great potential as visible light-sensitive photocatalysts [181, 195, 208-209].

Despite their advantages, metal sulfides face challenges as photocatalysts, such as high recombination rates of photogenerated carriers and susceptibility to photocorrosion To address these issues, loading cocatalysts onto metal sulfides is an effective strategy. Cocatalysts help suppress the recombination of photogenerated carriers, enhance the photocatalytic activity of composite materials, and reduce the activation energy of the reaction, thereby improving the overall performance [165].

Selenium-based chalcogenides are semiconductors that exhibit high light absorption coefficients, exceeding 10^4 cm^{-1} in the visible spectrum. Their band gap typically ranges from 1.8 to 2.0 eV [210]. Metal selenides offer several advantages as catalysts compared to metal sulfides, such as increased stability, lower cost, and improved photocatalytic performance. This increase in efficiency can be explained by the close energy levels of the 3d orbital of selenium with the 3s and 3p orbitals, which results in a stronger bond between the metal and selenium atoms. This bond strength may contribute to the higher stability and better catalytic properties of metal selenides compared to their sulfide counterparts [165]. When selenium is incorporated into metal catalysts, they acquire metallic properties that facilitate electron transfer and increase the likelihood of reaction pathways

resembling those observed in metal sulfide catalysts.

In recent years, the following compounds can be classified as selenide cocatalysts: Ni-Se [211-214], Co-Se [215-216], Zn-Se [184, 217-220], Sb-Se [217-225], Mo-Se [226-229], W-Se [230-231], Ag-Se [232], Fe-Se [233] and In-Se [234]. The lower Se-H_{ads} binding energy (273 kJ/mol^{-1}), which is closer to the Pt-H_{ads} binding energy (251 kJ/mol^{-1}), makes selenium-based cocatalysts an attractive alternative to amorphous and sulfur-rich cocatalysts for photoelectrochemical hydrogen production [235, 236].

Based on recent theoretical calculations, it has been found that the energy required to adsorb hydrogen on nickel selenide sites is similar to that required to adsorb hydrogen on platinum (Pt) sites, which are widely recognized as the most efficient cocatalysts for hydrogen evolution. This discovery suggests that nickel selenide could potentially replace platinum as a less expensive alternative for this reaction [237, 238]. Researchers have studied the use of nickel selenide-based cocatalysts such as $NiSe_{1+x}$, $NiSe_2$, and $NiSe_x$ for efficient photocatalytic hydrogen evolution reaction. Also, in [239], promising results were shown using amorphous $NiSe_{1+x}$ nanodots as a cocatalyst for TiO_2 photocatalysts.

While $MoSe_2$ has been identified as a potential cocatalyst for the photoelectrochemical hydrogen evolution reaction due to its lower Gibbs free energy compared to MoS_2, there are limited studies investigating its role in this context [240, 241]. $MoSe_2$ can assume two distinct phases: a metastable metallic phase 1T and a more stable semiconducting phase 2H, depending on the arrangement of the Se atoms. The semiconducting phase 2H of $MoSe_2$ exhibits intrinsic photocatalytic activity. However, recent studies indicate that the metallic phase of 1T $MoSe_2$ may have superior performance for photoelectrochemical hydrogen evolution. This is due to the greater accessibility of the reactive sites of the metallic phase 1T on both the basal and edge planes, as well as its superior metallic electron conductivity, potentially leading to improved photoelectrocatalytic performance in the hydrogen evolution reaction [196, 242-243].

Metal selenides are promising photocatalytic cocatalysts for hydrogen production due to their unique properties. They offer advantages such as stability, cost-effectiveness, and improved performance compared to metal sulfides. Nickel selenide, in particular, has potential as a lower-cost alternative to platinum. Amorphous and selenium-enriched cocatalysts have also demonstrated significant improvements in photocatalytic activity. Combining metal selenides with other semiconductors improves charge transport. However, further research is needed to optimize selenide-enriched cocatalysts and develop reliable synthesis methods. Progress in this area will facilitate the development of efficient and stable photocatalysts for hydrogen production [196].

Tellurium-based chalcogenides are less studied than their S- and Se-based counterparts, mainly due to their higher cost and lower stability [244]. However, the bond strength of Te-H atoms (238 kJ·mol^{-1}) is similar to that of Pt-H atoms (251 kJ·mol^{-1}), which makes them a potential alternative to Pt as a cocatalyst for photoelectrochemical hydrogen evolution, since the bond strength of Te-H atoms is comparable to that of Pt-H, which is commonly used as a cocatalyst due to its high bond strength. The bond strength of Se-H atoms (273 kJ·mol^{-1}) and S-H atoms (363 kJ·mol^{-1}) is higher than that of Te-H atoms, but lower than that of Pt-H atoms [245]. Transition metal tellurides such as $MnTe_x$ [246-247], $MoTe_2$ [248-252], $NiTe_x$ [253-256], ZnTe [257-258], $CdTe_x$ [259-261], Bi_2Te_3 [262-263], and $Co_{1.67}Te_2$ [261] have attracted considerable attention due to their exceptional optical properties, high proton adsorption capacity, and high electrical conductivity. These materials are widely used in various applications, including solar cells, optoelectronic devices, and photoelectrocatalysts for splitting water to produce hydrogen [265, 266]. Their distinctive properties make them ideal for a variety of applications. These materials exhibit direct band gaps, high transparency, and high absorption coefficients. Furthermore, according to theoretical studies, the unique p–π electron distribution of these catalysts creates electrically sensitive Te active sites, which are highly efficient in activating water molecules. This property is a result of the special concentration of p–π electrons of the active centers of Te exposed to metal telluride [267, 268].

Among metal tellurides, ZnTe is a semiconductor material with a small band gap of about 2.23-2.30 eV, which allows it to absorb visible light over a wide range [269]. Thanks to this property, it is capable of forming p-n heterostructures with other semiconductor materials. Moreover, the narrow band gap of ZnTe facilitates efficient separation of photogenerated electrons and holes, making it a highly promising material for various photocatalytic applications. Efficient interfacial electron transfer between semiconductors is facilitated by ZnTe among p-type semiconductors, making it a key driving force for photocatalytic activity. Research has already demonstrated the potential of ZnTe as a photocatalytic material, and its broad visible light absorption spectrum makes it a promising candidate for future applications in this field [270].

In general, metal tellurides show promise as catalysts and cocatalysts for photocatalytic hydrogen evolution. They have bond strength comparable to platinum, as well as favorable optical properties and high conductivity. Recent research has focused on enhancing the performance of transition metal chalcogenides through techniques such as heterojunction design and modification [196]. The incorporation of transition metal chalcogenides into other semiconductors improves charge transport and enhances photocatalytic activity. Further research is aimed at optimizing the synthesis methods, studying different compositions of transition metal chalcogenides, and investigating their long-term stability and performance. Metal tellurides can make a significant contribution to the development of efficient and environmentally friendly methods for producing hydrogen [196].

Phosphides, another class of two-dimensional layered materials, are among the promising candidates due to their unique properties and potential applications in various fields. Like transition metal chalcogenides, phosphides consist of transition metal atoms covalently bonded to phosphorus atoms, with individual layers held together by van der Waals forces. Phosphides exhibit unique properties, including high electron mobility, a tunable band gap, and strong light absorption in the visible spectrum, making them promising candidates for optoelectronic and photovoltaic devices [196, 271]. Furthermore, phosphides have shown potential for catalytic applications due to their large surface area and unique electronic structure [272]. The use of noble metal-based catalysts in photocatalytic hydrogen production is limited by their rarity and high cost, necessitating the development of alternative, more accessible, and more efficient options. As a result, there is a growing demand for the development of photocatalysts without precious metals. Recently, transition metal phosphides, which are abundant on Earth, have been considered as promising candidates for HER due to their low cost and high efficiency. This development is particularly important given the growing demand for sustainable and cost-effective methods of hydrogen production [273-276].

Photoelectrocatalytic hydrogen production often involves the use of transition metal phosphides such as FeP_x, CoP_x, and NiP_x as cocatalysts [195, 277]. In addition, CuP_x, MoP_x, WP_x, and bimetallic phosphides were also found to be effective cocatalysts in this process [195, 278].

The use of iron phosphides as catalysts in photoelectrocatalytic hydrogen production is gaining popularity due to their high availability, cost-effectiveness, and the presence of active iron-containing clusters, which are also found in catalysts for biohydrogen evolution. Considerable research has been conducted on iron phosphides, and they have been used in widespread application as cocatalysts in photoelectrocatalytic hydrogen production systems [279-281]. These studies showed that the use of FeP and Fe_2P cocatalysts can greatly enhance the efficiency of photoelectrocatalytic hydrogen production. However, most of these studies used FeP or Fe_2P nanoparticles, which are prone to aggregation, reducing the number of available active sites. To further improve the performance of photoelectrocatalytic hydrogen production, further research is needed to develop various nanostructured iron phosphides, such as 0D and 2D ultrafine nanoparticles with higher active site density [195].

The excellent catalytic properties of various cobalt phosphides for H_2 production via photocatalysis have attracted considerable attention. Although remarkable progress has been made in improving photoexcited charge separation and photocatalytic activity, a

complete understanding of the interface interactions and chemical bonds between cobalt phosphide-based cocatalysts and semiconductor photocatalysts is still lacking. Although some studies have explored the correlation between chemical bonds and photocatalytic efficiency, research in this area has been limited to a few recent investigations. These studies highlight the potential of cobalt phosphides as promising cocatalysts for photoelectrocatalytic hydrogen production, primarily due to their tunable nanostructure. However, in many cases, the incorporation of nanostructured cobalt phosphides into semiconductors is achieved by the post-loading method, which often leads to weakening of the interfacial contact between the cobalt phosphides and the semiconductors. In this regard, it is extremely important for future research to prioritize the development of methods that ensure strong and tight interaction of nanostructured cobalt phosphides with semiconductors, which will reduce the Schottky barrier [195]. Ni_2P and $Ni_{12}P_5$ have become key materials in the nickel phosphide family, serving as efficient cocatalysts for photoelectrocatalytic hydrogen production. Their exceptional stability and activity make them particularly attractive for such applications. Researchers have developed innovative nanostructures to enhance the interaction between the Ni_2P cocatalyst and semiconductor photocatalysts, thereby accelerating the movement of photoexcited charges. This strategy has the potential to improve the efficiency of photocatalytic reactions by promoting the separation and transfer of electrons and holes generated by light absorption [282-283]. In addition, to meet the demands of practical applications, Ni_2P has been integrated into various complex photoelectrocatalytic hydrogen production systems. Despite seawater accounting for 97% of the Earth's water resources, achieving efficient photoelectrocatalytic hydrogen production from seawater remains challenging due to the presence of various cations and microorganisms.

To address this issue, the authors developed a photocatalytic system by loading carbon-encapsulated Ni_2P onto a fully delocalized organic polymer (COP-TF@CNi_2P), resulting in efficient and stable H_2 production via seawater decomposition [284]. Although the photocatalytic activity of nickel phosphides for photoelectrocatalytic hydrogen production has been extensively studied, most studies have focused primarily on the Ni_2P phase, ignoring other phases. Furthermore, the nickel-to-phosphorus ratio in these materials significantly influences their efficiency in photocatalytic hydrogen production. Therefore, further research is needed to explore the relationship between different nickel phosphide phases and their performance in photocatalytic hydrogen production. Such studies will be crucial for the advancement of this field [195].

The researchers also identified Cu_3P as a promising p-type cocatalyst for highly efficient photoelectrocatalytic hydrogen production. This discovery is particularly important because of the abundant availability of copper, an element widely distributed on Earth [285]. The authors fabricated a p–n junction by loading Cu_3P onto CdS nanorods [286]. The purpose of this arrangement was to improve charge transfer and increase the efficiency of photoelectrocatalytic hydrogen production. Scientists have successfully optimized the Cu_3P/CdS configuration, resulting in an impressive photocatalytic hydrogen production rate of approximately 200 $\mu mol \cdot h^{-1} \cdot mg^{-1}$ under visible-light irradiation [286].

Molybdenum phosphides (MoP) and tungsten phosphides (WP) have been identified as promising cocatalysts for efficient photoelectrocatalytic hydrogen production due to their abundance in the Earth's crust. Several studies have established the potential of these compounds for efficient hydrogen evolution [35, 287, 288].

Conclusion

The development of efficient photocatalysts with high photoconversion efficiency is the ultimate goal of photocatalytic hydrogen production. The review summarizes some typical approaches to the development of high-performance photocatalysts that aim to enhance photoconversion efficiency and presents fundamental aspects of scientific problems of solar-driven water splitting. Essentially, to achieve self-splitting water decomposition using

a single semiconductor, the band gap must cover the reduction and oxidation potentials of water so that photoexcited electrons and holes possess enough energy for hydrogen and oxygen evolution reactions, respectively. Wide bandgap semiconductors, such as TiO_2, are inexpensive and stable, but they are inefficient at harvesting sunlight due to their limited absorption in the visible spectrum. Although α-Fe_2O_3 and $BiVO_4$ have broader absorption than TiO_2, the photocurrents achieved for these materials do not achieve theoretical maximums. The main limiting factors are rapid carrier recombination and poor surface oxygen evolution reaction kinetics. Narrow-gap semiconductors such as CdS and III–V compounds have the potential to achieve high efficiency but suffer from instability over extended periods. The unique electronic and structural properties of transition metal chalcogenides and phosphides enable efficient separation and transport of electrons and holes, leading to increased generation rates of hydrogen. Furthermore, the band gap of these materials can be tuned by changing their composition or structure, which provides flexibility in optimizing their photocatalytic performance for specific applications. In addition, the use of these materials as cocatalysts further enhances their effectiveness in hydrogen release. Although transition metal chalcogenides and phosphides have demonstrated promising performance as photocatalysts for hydrogen evolution, several limitations and challenges remain to be addressed. One of the major problems is the low conductivity and limited ability of some photocatalysts to absorb light, which can significantly affect their efficiency. To address this issue, future research should focus on developing photocatalysts with enhanced electronic properties, such as higher electron mobility and better light absorption ability.

Furthermore, the environmental friendliness and feasibility of large-scale production of these photocatalysts must be considered. Some synthesis methods reported in previous studies are complex and costly, which may limit their practical application. Therefore, future research should focus on developing efficient and stable photocatalysts using synthesis methods that are both easily scalable and environmentally friendly.

However, despite significant advancements in developing photocatalysts with high conversion efficiency, several unresolved challenges still exist. For example, most heterojunctions based on metal chalcogenides are capable of splitting water only in the presence of agents. Therefore, it is crucial to develop new metal chalcogenide-based heterojunctions that can split water directly, without agents. There are two solutions: (1) combining two semiconductors in a heterojunction for both hydrogen and oxygen production; (2) developing and producing new metal chalcogenides with more suitable band gaps and potential band positions. Another problem for metal chalcogenides is that photocatalytically active sites for H_2 are rarely investigated. However, catalytic centers are very important for us to continue research on catalyst modification and efficiency improvement.

The ultimate goal of all solar fuel research is to develop and produce cost-effective, highly efficient, and stable photoanodes and/or photocathodes for the production of oxygen and/or hydrogen using either particle-based systems or photoelectrochemical devices.

References

1. Zhong Sh., Xi Y., Chen Q., Chen J., Bai S. Bridge engineering in photocatalysis and photoelectrocatalysis. *Nanoscale*, 2020, **Vol. 12(10)**, p. 5764-5791. DOI: 10.1039/C9NR10511E !
2. Coha M., Farinelli G., Tiraferri A., Minella M., Vione D. Advanced oxidation processes in the removal of organic substances from produced water: Potential, configurations, and research needs. *Chem. Eng. J.,* 2021, Vol. 414, 128668. DOI: 10.1016/j.cej.2021.128668.
3. Szklarczyk M. *Photoelectrocatalysis.* In: Murphy O.J., Srinivasan S., Conway B.E. (eds) Electrochemistry in Transition. Springer. Boston, MA. 1992. DOI: 10.1007/978-1-4615-9576-2_15
4. Bessegato G.G., Guaraldo T.T., de Brito J.F., Brugnera M.F., Boldrin Zanoni M.V. Achievements and Trends in Photoelectrocatalysis: from Environmental to

Energy Applications. *Electrocatalysis*, 2015, **Vol. 6**, p. 415–441. DOI: 10.1007/s12678-015-0259-9
5. Bard A.J. Photoelectrochemistry. *Science*, 1980, **Vol. 207(4427)**, p. 139-144. DOI: 10.1126/science.207.4427.13
6. Daghrir R. Drogui P. Robert D. Photoelectrocatalytic technologies for environmental applications. *Journal of Photochemistry and Photobiology A: Chemistry*, 2012, **Vol. 238**, p. 41-52. DOI: 10.1016/j.jphotochem.2012.04.009
7. Linsebigler A.L., Lu G.Q., Yates J.T. Photocatalysis on TiO_2 Surfaces-Principles, Mechanisms, and Selected Results. *Chemical Reviews*, 1995, **Vol. 95(3)**, p. 735-58. DOI: 10.1021/cr00035a013
8. Bessegato G.G., Guaraldo T.T., Zanoni M.V.B. *Enhancement of Photoelectrocatalysis Efficiency by Using Nanostructured Electrodes*. Modern Electrochemical Methods in Nano, Surface and Corrosion Science. 2014, p. 271-319. DOI:10.5772/58333
9. Gao C., Wang J., Xu H., Xiong Y. Coordination chemistry in the design of heterogeneous photocatalysts. *Chem. Soc. Rev.*, 2017, **Vol. 46(10)**, p. 2799–2823. DOI: 10.1039/C6CS00727A
10. Tong H., Ouyang S., Bi Y., Umezawa N., Oshikiri M., Ye J. Nano-photocatalytic Materials: Possibilities and Challenges. *Adv. Mater.*, 2012, **Vol. 24(2)**, p. 229–251. DOI: 10.1002/adma.201102752
11. Jiang C., Moniz S.J.A., Wang A., Zhang T., Tang J. Photoelectrochemical devices for solar water splitting – materials and challenges. *Chem. Soc. Rev.,* 2017, **Vol. 46(15)**, p. 4645–4660. DOI: 10.1039/C6CS00306K
12. Liu R., He G., Su Y., Ding D. Solar energy for low carbon buildings: choice of systems for minimal installation area, cost, and environmental impact. *City Built Enviro,* **Vol. 1**, 2023, 16. DOI: 10.1007/s44213-023-00019-8
13. Alayi R., Khalilpoor N., Heshmati S., Najafi A., Issakhov A. Thermal and Environmental Analysis Solar Water Heater System for Residential Buildings. *International Journal of Photoenergy*, 2021, Article ID 6838138, 9 pages. DOI: 10.1155/2021/6838138
14. Meena Ch.S., Prajapati A.N., Kumar A., Kumar M. Utilization of Solar Energy for Water Heating Application to Improve Building Energy Efficiency: An Experimental Study. *Buildings,* 2022, **Vol. 12(12)**, 2166. DOI: 10.3390/buildings12122166
15. Zeeshan, Panigrahi B.K., Ahmed R., Mehmood M.U., Park J.Ch., Kim Y., C hun W. Operation of a low-temperature differential heat engine for power generation via hybrid nanogenerators. *Applied Energy*, 2021, **Vol. 285**, 116385. DOI: 10.1016/j.apenergy.2020.116385
16. Aydogan H., Ozcelık A.E., Acaroglu M., Işık H. A Study on Generating Electricity by Using Exhaust Waste Heat in a Diesel Engine. *Applied Mechanics and Materials*, 2014, **Vols. 446-447**, p. 858-862. DOI:10.4028/www.scientific.net/AMM.446-447.858
17. Tatishvili G., Aliyev A., Bolashvili N., Tsatsanashvil i M., Nioradze N., Kvinikadze L. Green hydrogen energy prospects: Georgia - Azerbaijan strategic partnership. *International Journal of Hydrogen Energy*, 2025, **Vol. 193**, 152258. DOI: 10.1016/j.ijhydene.2025.152258
18. Aliyev A.Sh., Elrouby M., Cafarova S.F. Electrochemical synthesis of molybdenum sulfide semiconductor. *Materials science in semiconductor processing*, 2015, **Vol. 32**, p. 31-39. DOI: 10.1016/j.mssp.2015.01.006
19. Gurevich Yu.Ya., Pleskov Yu.V. *Photoelectrochemistry of semiconductors*. M. Nauka. 1983. 312 p.
20. Murphy A.B., Barnes P.R.F., Randeniya L.K., Plumb I.C., Grey I.E., Horne M.D., Glasscock J.A. Efficiency of solar water splitting using semiconductor electrodes. *International Journal of Hydrogen Energy*, 2006, **Vol. 31(14)**, p. 1999-2017. DOI: 10.1016/j.ijhydene.2006.01.014
21. Jia J., Seitz L.C., Benck J.D., Huo Y., Chen Y., Ng J.W.D., Bilir T., Harris J.S., Jaramillo T.F. Solar water splitting by photovoltaic-electrolysis with a solar-to-hydrogen efficiency over 30%. *Nature Communications*, 2016, **Vol. 7**,

Article number: 13237. DOI: 10.1038/ncomms13237
22. Sportelli G., Marchi M., Fornasiero P., Filippini G., Franco F., Melchionna M. Photoelectrocatalysis for Hydrogen Evolution Ventures into the World of Organic Synthesis. *Global Challenges*, 2024, **Vol. 8(6)**, 2400012. DOI:10.1002/gch2.202400012
23. Ahmed M., Dincer I. A review on photoelectrochemical hydrogen production systems: Challenges and future directions. *International Journal of Hydrogen Energy*, 2019, **Vol. 44(5)**, p. 2474-2507. DOI: 10.1016/j.ijhydene.2018.12.037
24. Alexander B.D., Kulesza P.J., Rutkowska I., Solarskac R., Augustynski J. Metal oxide photoanodes for solar hydrogen production. *J. Mater. Chem.*, 2008, **Vol. 18(20)**, p. 2298-2303. DOI: 10.1039/B718644D
25. Liu B., Wang Sh., Zhang G., Gong Z., Wu B., Wang T., Gong J. Tandem cells for unbiased photoelectrochemical water splitting. *Chem. Soc. Rev.*, 2023, **Vol. 52**, p. 4644-4671. DOI: 10.1039/D3CS00145H
26. Lee M., Haas S., Smirnov V., Merdzhanova T., Rau U. Scalable Photovoltaic-Electrochemical Cells for Hydrogen Production from Water - Recent Advances. *ChemElectroChem*, 2022, **Vol. 9(24)**, e202200838, 21 pages. DOI: 10.1002/celc.202200838
27. Sivula K., van de Krol R. Semiconducting materials for photoelectrochemical energy conversion. *Nat Rev Mater* 2016, **Vol. 1**, 15010. DOI: 10.1038/natrevmats.2015.10
28. Ye Sh., Shi W., Liu Y., Li D., Yin H., Chi H., Luo Y., Ta N., Fan F., Wang X., Li C. Unassisted Photoelectrochemical Cell with Multimediator Modulation for Solar Water Splitting Exceeding 4% Solar-to-Hydrogen Efficiency. *J. Am. Chem. Soc*. 2021, **Vol. 143(32)**, p. 12499–12508. DOI: 10.1021/jacs.1c00802
29. Garcia-Navarro J., Isaacs M.A., Favaro M., Ren D., Ong W., Grätzel M., Jiménez-Calvo P. Updates on Hydrogen Value Chain: A Strategic Roadmap, *Global Challenges,* 2023, **Vol. 8(6)**, 2300073. DOI: 10.1002/gch2.202300073
30. Lee M., Haas S., Smirnov V., Merdzhanova T., Rau U. Scalable Photovoltaic-Electrochemical Cells for Hydrogen Production from Water - Recent Advances. *ChemElectroChem,* 2022, **Vol. 24(9)**, 202200838. DOI: 10.1002/celc.202200838
31. Jian J., Jiang G., Van De Krol R., Wei B., Wang H. Recent advances in rational engineering of multinary semiconductors for photoelectrochemical hydrogen generation. *Nano Energy,* 2018, **Vol. 51**, p. 457-480. DOI: 10.1016/j.nanoen.2018.06.074
32. Guevarra D., Shinde A., Suram S.K., Sharp I.D., Toma F.M., Haber J.A., Gregoire J.M. Development of solar fuels photoanodes through combinatorial integration of Ni-La-Co-Ce oxide catalysts on $BiVO_4$. *Energy Environ. Sci.* 2016, **Vol. 9(2)**, p. 565-580. DOI:10.1039/c5ee03488d
33. Bassi P.S., Antony R.P., Boix P.P., Fang Y., Barber J., Wong L.H. Crystalline Fe_2O_3/Fe_2TiO_5 heterojunction nanorods with efficient charge separation and hole injection as photoanode for solar water oxidation. *Nano Energy,* 2016, **Vol. 22**, p. 310-318. DOI:10.1016/j.nanoen.2016.02.013
34. Shanmugaratnam S., Yogenthiran E., Koodali R., Ravirajan P., Velauthapillai D., Shivatharsiny Y. Recent Progress and Approaches on Transition Metal Chalcogenides for Hydrogen Production. *Energies,* 2021, **Vol. 14(24)**, 8265. DOI: 10.3390/en14248265
35. Cheng Ch., Zong Sh., Shi J., Xue F., Zhang Y., Guan X., Zheng B., Deng J., Guo L. Facile preparation of nanosized MoP as cocatalyst coupled with g-C_3N_4 by surface bonding state for enhanced photocatalytic hydrogen production. *Applied Catalysis B: Environmental*, 2020, Vol. 265, 118620. DOI: 10.1016/j.apcatb.2020.118620
36. Makwana N.M., Tighe C.J., Gruar R.I., McMillan P.F., Darr J.A. Pilot plant scale continuous hydrothermal synthesis of nano-titania; effect of size on photocatalytic activity. *Mater. Sci. Semicond. Process.* 2016, **Vol. 42**, p. 131–137. DOI: 10.1016/j.mssp.2015.08.043

37. Huerta-Flores A.M., Torres-Martínez L.M., Moctezuma E., Singh A.P., Wickman B. Green synthesis of earth-abundant metal sulfides (FeS_2, CuS, and NiS_2) and their use as visible-light active photocatalysts for H_2 generation and dye removal. *J. Mater. Sci. Mater. Electron.* 2018, **Vol. 29**, p. 11613–11626. DOI: 10.1007/s10854-018-9259-x
38. Yu J., Xu C., Ma F., Hu, S.-P.; Zhang, Y.-W.; Zhen, L. Monodisperse SnS_2 Nanosheets for High-Performance Photocatalytic Hydrogen Generation. *ACS Appl. Mater. Interfaces.* 2014, **Vol. 6**, p. 22370–22377. DOI: 10.1021/am506396z
39. Xu K., Wang F., Wang Z., Zhan X., Wang Q., Cheng Z., Safdar M., He J. Component-Controllable $WS_{2(1-x)}Se_{2x}$ Nanotubes for Efficient Hydrogen Evolution Reaction. *ACS Nano,* 2014, **Vol. 8**, p. 8468–8476. DOI: 10.1021/nn503027k
40. Voiry D., Salehi M., Silva R., Fujita T., Chen M., Asefa T., Shenoy V.B., Eda G., Chhowalla M. Conducting MoS_2 Nanosheets as Catalysts for Hydrogen Evolution Reaction. *Nano Lett.* 2013, **Vol. 13**, p. 6222–6227. DOI: 10.1021/nl403661s
41. Wang Y., Yang X., Wang Z., Lv X., Jia H., Kong J., Yu M. CdS and SnS_2 nanoparticles co-sensitized TiO_2 nanotube arrays and the enhanced photocatalytic property. *J. Photochem. Photobiol. Chem.* 2016, **Vol. 325**, p. 55–61. DOI: 10.1016/j.jphotochem.2016.04.008
42. Wang Q., Huang J., Sun H., Ng Y.H., Zhang K.-Q., Lai Y. MoS_2 Quantum Dots@TiO_2 Nanotube Arrays: An Extended-Spectrum-Driven Photocatalyst for Solar Hydrogen Evolution. *ChemSusChem,* 2018, **Vol. 11**, p. 1708–1721. DOI: 10.1002/cssc.201800379
43. Sun Y., Liu C., Grauer D.C., Yano J., Long J.R., Yang P., Chang C.J. Electrodeposited Cobalt-Sulfide Catalyst for Electrochemical and Photoelectrochemical Hydrogen Generation from Water. *J. Am. Chem. Soc.* 2013, **Vol. 135**, p. 17699–17702. DOI: 10.1021/ja4094764
44. Li Y., Wang H., Peng S. Tunable Photodeposition of MoS_2 onto a Composite of Reduced Graphene Oxide and CdS for Synergic Photocatalytic Hydrogen Generation. *J. Phys. Chem. C,* 2014, **Vol. 118**, p. 19842–19848. DOI: 10.1021/jp5054474
45. Wang Q., Lei Y., Wang Y., Liu Y., Song C., Zeng J., Song Y., Duan X., Wang D., Li Y. Atomic-scale engineering of chemical-vapor-deposition-grown 2D transition metal dichalcogenides for electrocatalysis. *Energy Environ. Sci.* 2020, **Vol. 13**, p. 1593–1616. DOI: DOI: 10.1039/D0EE00450B
46. Wang Y., Li L., Yao W., Song S., Sun J.T., Pan J., Ren X., Li C., Okunishi E., Wang Y.-Q., Wang E., Shao Y., Zhang Y. Y., Yang H., Schwier E.F., Iwasawa H., Shimada K., Taniguchi M., Cheng Zh., Zhou Sh., Du Sh., Pennycook S.J., Pantelides S.T., Gao H.-J. Monolayer $PtSe_2$, a New Semiconducting Transition-Metal-Dichalcogenide, Epitaxially Grown by Direct Selenization of Pt. *Nano Lett.* 2015, **Vol. 15**, p. 4013–4018. DOI: 10.1021/acs.nanolett.5b00964
47. Sarwar S., Nautiyal A., Cook J., Yuan Y., Li J., Uprety S., Shahbazian-Yassar R., Wang R., Park M., Bozack M.J., Zhang X. Facile microwave approach towards high performance MoS_2/graphene nanocomposite for hydrogen evolution reaction. *Sci. China Mater.* 2020, **Vol. 63**, p. 62–74. DOI: 10.1007/s40843-019-9555-0
48. Jiao F., Yen H., Hutchings G.S., Yonemoto B., Lua Q., Kleitz F. Synthesis, structural characterization, and electrochemical performance of nanocast mesoporous Cu-/Fe-based oxides. *J. Mater. Chem. A,* 2014, **Vol. 2**, p. 3065–3071. DOI: https://doi.org/10.1039/C3TA14111J
49. Panigrahi P.K., Pathak A. Microwave-assisted synthesis of WS_2 nanowires through tetrathiotungstate precursors. *Sci. Technol. Adv. Mater.* 2008, **Vol. 9**, 045008. DOI: 10.1088/1468-6996/9/4/045008
50. Liu H., Su Y., Chen P., Wang Y. Microwave-assisted solvothermal synthesis of 3D carnation-like SnS_2 nanostructures with high visible light photocatalytic activity. *J. Mol. Catal. Chem.* 2013, Vol. 378, p. 285–292. DOI: 10.1016/j.molcata.2013.06.021
51. Xu H., Ouyang Sh., Liu L., Reunchan P., Umezawaace N., Ye J. Recent advances in

TiO_2-based photocatalysis. *Journal of Materials Chemistry A: Materials for Energy and Sustainability*, 2014, **Vol. 2(32)**, p. 12642-12661. DOI: 10.1039/c4ta00941j

52. Abdullayeva S., Eminov Sh., Jalilova Kh., Musayeva N., Guliyev J., Aliyev A., Majidzade V., Mammadova G. Synthesis of anodic TiO_2 nanotubes on indium tin oxide coated glass electrodes. *International Journal of Energy Research*, 2022, **Vol. 46(15)**, p. 21686-21693. DOI: 10.1002/er.8667
53. Franz S., Arab H., Lucotti A., Castiglioni Ch., Vicenzo A., Morini F., Bestetti M. Exploiting Direct Current Plasma Electrolytic Oxidation to Boost Photoelectrocatalysis. *Catalysts,* 2020, **Vol. 10(3)**, 325. DOI: 10.3390/catal10030325
54. Piskunov S., Lisovski O., Begens J., Bocharov D., Zhukovskii Y.F., Wessel M., Spohr E. C-, N-, S-, and Fe-Doped TiO_2 and $SrTiO_3$ Nanotubes for Visible-Light-Driven Photocatalytic Water Splitting: Prediction from First Principles. *Journal of Physical Chemistry C*, 2015, **Vol. 119(32)**, p. 18686–18696. DOI: 10.1021/acs.jpcc.5b03691
55. Chen X., Liu L., Yu P.Y., Mao S.S. Increasing Solar Absorption for Photocatalysis with Black Hydrogenated Titanium Dioxide Nanocrystals. *Science,* 2011, **Vol. 331(6018)**, p. 746-750. DOI: 10.1126/science.1200448
56. Sawal M.H., Jalil A.A., Khusnun N.F., Hassan N.S., Bahari M.B. A review of recent modification strategies of TiO_2-based photoanodes for efficient photoelectrochemical water splitting performance. *Electrochimica Acta*, 2023, **Vol. 467**, 143142. DOI: 10.1016/j.electacta.2023.143142
57. Zhang Y., Niu J., Zhao J., Zou J., Chang B., Shi F., Cheng H. Influence of exponential-doping structure on photoemission capabilityof transmission-mode GaAs photocathodes. *Journal of Applied Physics*, 2010, **Vol. 108**, 093108. DOI:10.1063/1.3504193
58. Sivula K., Le Formal F., Grätzel M. Solar Water Splitting: Progress Using Hematite (α-Fe_2O_3) Photoelectrodes. *ChemSusChem*, 2011, **Vol. 4(4),** p. 432-449. DOI:10.1002/cssc.201000416
59. Jiang Ch., Moniz S.O. A., Wang A., Zhang T., Tang J. Photoelectrochemical devices for solar water splitting – materials and challenges. *Chem. Soc. Rev.*, 2017, **Vol. 46**, p. 4645-4660. DOI: 10.1039/C6CS00306K
60. van de Krol R., Liang Y., Schoonman J. Solar hydrogen production with nanostructured metal oxides. *J. Mater. Chem*., 2008, **Vol. 18**, p. 2311–2320. DOI: 10.1039/b718969a
61. Steier L., Herraiz-Cardona I., Gimenez S., Fabregat-Santiago F., Bisquert J., Tilley S.D., Grätzel M. Understanding the Role of Underlayers and Overlayers in Thin Film Hematite Photoanodes. *Adv. Funct. Mater.*, 2014, **Vol. 24**, p. 7681 —7688. DOI: 10.1002/adfm.201402742
62. Peerakiatkhajohn P., Yun J.-H., Chen H., Lyu M., Butburee T., Wang L. Stable Hematite Nanosheet Photoanodes for Enhanced Photoelectrochemical Water Splitting. *Adv. Mater.*, 2016, **Vol. 28**, p. 6405 —6410. DOI: 10.1002/adma.201601525
63. Patterer L., Mayer E.B., Stanislav M., Pöllmann P.J., Hans M., Primetzhofer D., Souza Filho I.R., Springer H.J., Schneider J.M. Effect of Si on the hydrogen-based direct reduction of Fe_2O_3 studied by XPS of sputter-deposited thin-film model systems. *Scripta Materialia,* 2023, **Vol. 233**, 115515. DOI: 10.1016/j.scriptamat.2023.115515
64. Maivroides J.G., Kafalas J.A., Kolesar D.F. Photoelectrolysis of water in cells with $SrTiO_3$ anodes. *Applied Physics Letters*, 1976, **Vol. 28**, p. 241–243. DOI: 10.1063/1.88723
65. Tinnemans A.H.A., Mackor A. Spectral sensitization of $SrTiO_3$ photoanodes with binuclear 1,10-phenantroline bis(2,2'-bipyridine) complexes of ruthenium(II) and tris-(2,2'-bipyridine) ruthenium (II). *Recueil des Traveaux Chimiques des Pays-Bas*, 1981, **Vol. 100(7-8),** p. 295–296. DOI: 10.1002/recl.19811000712
66. Kornblum L., Fenning D.P., Faucher J., Hwang J., Boni A., Han M.G., Morales-Acosta M. D., Zhu Y., Altman E.I., Lee M.L., Ahn C.H., Walker F.J., Shao-Horn Y. Solar

hydrogen production using epitaxial $SrTiO_3$ on a GaAs photovoltaic. *Energy Environ. Sci.*, 2017, **Vol. 10(1)**, p. 377-382. DOI: 10.1039/C6EE03170F

67. Lucas T.T.A., Melo M.A., Freitas A.L.M., Souza F.L., Gonçalves R.V. Enhancing the solar water splitting activity of TiO_2 nanotube-array photoanode by surface coating with La-doped $SrTiO_3$. *Solar Energy Materials and Solar Cells*, 2020, **Vol. 208,** 110428. DOI: 10.1016/j.solmat.2020.110428
68. Maeda K. Rhodium-doped barium titanate perovskite as a stable p-type semiconductor photocatalyst for hydrogen evolution under visible light. *ACS Appl. Mater. Interfaces*, 2014, **Vol. 6(3),** p. 2167-2173. DOI: 10.1021/am405293e
69. Lin X., Xing J., Wang W., Shan Z., Xu F., Huang F. Photocatalytic activities of heterojunction semiconductors Bi_2O_3/$BaTiO_3$: a strategy for the design of efficient combined photocatalysts. *J. Phys. Chem. C*, 2007, **Vol. 111(49),** p. 18288-18293. DOI: 10.1021/jp073955d
70. Meng J., Lin Q., Wu S., Pei J., Wei X., Li J., Zhang Z. Hybrid CN-MEA microplates with enhanced photocatalytic hydrogen evolution under visible light irradiation. *Catal. Sci. Technol.*, 2017, **Vol. 7(17),** p. 3777-3784. DOI: 10.1039/C7CY00572E
71. Zhang W.-D., Middendorf J.R., Brown E.R. Demonstration of a GaAs-based 1550-nm continuous wave photomixer. *Appl. Phys. Lett.* 2015, **Vol. 106**, 021119. DOI: 10.1063/1.4906284
72. Ren P., Fan H., Wang X. Electrospun nanofibers of ZnO/$BaTiO_3$ heterostructures with enhanced photocatalytic activity. *Catal. Commun.*, 2012, **Vol. 25**, p. 32-35. DOI: 10.1016/j.catcom.2012.04.003
73. Yang W., Yu Y., Starr M.B., Yin X., Li Z., Kvit A., Wang S., Zhao P., Wang X. Ferroelectric polarization-enhanced photoelectrochemical water splitting in TiO_2–$BaTiO_3$ core–shell nanowire photoanodes. *Nano Lett.,* 2015, **Vol. 15(11),** p. 7574-7580. DOI: 10.1021/acs.nanolett.5b03988
74. Xian T., Yang H., Di L., Dai J. Enhanced photocatalytic activity of $BaTiO_3$@ g-C_3N_4 for the degradation of methyl orange under simulated sunlight irradiation. *J. Alloys Compd.*, 2015, Vol. 622(), p. 1098-1104. DOI: 10.1016/j.jallcom.2014.11.051
75. Augurio A., Alvarez-Fernandez A., Panchal V., Pittenger B., De Wolf P., Guldin S., Briscoe J. Controlled Porosity in Ferroelectric $BaTiO_3$ Photoanodes. *ACS Applied Materials & Interfaces,* 2022, **Vol. 14(11),** p. 13147–13157. DOI: 10.1021/acsami.1c17419
76. Liu J., Sun Y., Li Z. Ag loaded flower-like $BaTiO_3$ nanotube arrays: fabrication and enhanced photocatalytic property. *CrystEngComm*, 2012, **Vol. 14(4),** p. 1473-1478. DOI: 10.1039/C1CE05949A
77. Li L., Liu X., Zhang Y., Salvador P.A., Rohrer G.S. Heterostructured (Ba, Sr) TiO_3/TiO_2 core/shell photocatalysts: influence of processing and structure on hydrogen production. *Int. J. Hydrogen Energy*, 2013, **Vol. 38(17),** p. 6948-6959. DOI: 10.1016/j.ijhydene.2013.03.130
78. Fan H., Li H., Liu B., Lu Y., Xie T., Wang D. Photoinduced charge transfer properties and photocatalytic activity in Bi_2O_3/$BaTiO_3$ composite photocatalyst. *ACS Appl. Mater. Interfaces*, 2012, **Vol. 4(9),** p. 4853-4857. DOI: 10.1021/am301199v
79. Zhao Y., Ran L., Chen R., Song Y., Gao J., Sun L., Hou J. Boosting Charge Mediation in Ferroelectric $BaTiO_{3-x}$-Based Photoanode for Efficient and Stable Photoelectrochemical Water Oxidation. *Small Structure*, 2023, Vol. 4(9), 2300072. DOI: 10.1002/sstr.202300072
80. Feng Ch., Liu J., Zhang Y., Qian Y., Song Y., Bao Y., Zhao J. Comparison of photoemission performance of a GaAs photocathode between white light and monochromatic light illumination during. *Applied Optics*, 2019, **Vol. 58(32),** p. 8751-8756. DOI: 10.1364/AO.58.008751
81. Alqahtani M., Sathasivam S., Cui F., Steier L., Xia X., Blackman Ch., Kim E., Shin H., Benamara M., Mazur Y.I., Salamo G.J., Parkin I.P., Liu H., Wu J. Heteroepitaxy of GaP on Silicon for Efficient and Cost-Effective Photoelectrochemical Water Splitting. *J. Mater. Chem. A*, 2019, **Vol. 7(14)**, p. 8550-8558. DOI: 10.1039/C9TA01328H

82. Kudo A., Ueda K., Kato H., Mikami İ. Photocatalytic O_2 evolution under visible light irradiation on $BiVO_4$ in aqueous $AgNO_3$ solution. *Catalysis Letters,* 1998, **Vol. 53,** p. 229–230. DOI: 10.1023/A:1019034728816
83. Park Y., McDonald K.J., Choi K.-Sh. Progress in bismuth vanadate photoanodes for use in solar water oxidation. *Chem. Soc. Rev.*, 2013, **Vol. 42(6)**, p. 2321-2337. DOI: 10.1039/C2CS35260E
84. Pilli S.K., Furtak T.E., Brown L.D., Deutsch T.G., Turner J.A., Herring A.M. Cobalt-phosphate (Co-Pi) catalyst modified Mo-doped $BiVO_4$ photoelectrodes for solar water oxidation. *Energy Environ. Sci.*, 2011, **Vol. 4(12)**, p. 5028-5034. DOI: 10.1039/C1EE02444B
85. Abdi F.F., Han L., Smets A.H.M., Zeman M., Dam B., van de Krol R. Efficient solar water splitting by enhanced charge separation in a bismuth vanadate-silicon tandem photoelectrode. *Nat. Commun.*, 2013, **Vol. 4**, 2195. DOI: 10.1038/ncomms3195.
86. Bae J., Bazarov I., Cultrera L., Galdi A., Ikponmwen F., Maxson J. Enhanced robustness of GaAs-based photocathodes activated by Cs, Sb, and O_2. *North American Particle Acc. Conf.* 2019, p. 210-212. DOI: 10.18429/JACoW-NAPAC2019-MOPLH17
87. Clampin M., Paresce F. Photon-counting imaging with a GaAs photocathode - Evaluation of the Red-Ranicon for astronomical imaging. *Astronomy and Astrophysics*, 1989, **Vol. 225(2),** p. 578-584.
88. Calabrese R., Carugno G., Tecchio L. Generation of high-current electron bunches from a GaAs photocathode. *Detectors and Associated Equipment*, 1990, **Vol. 292(3)**, p. 728-730. DOI: 10.1016/0168-9002(90)90194-B
89. Chanlek N., Herbert J.D., Jones R.M., Jones L.B., Middleman K.J., Militsyn B.L. The degradation of quantum efficiency in negative electron affinity GaAs photocathodes under gas exposure. *J. Phys. D: Appl. Phys.,* 2014, **Vol. 47(5),** 055110. DOI: 10.1088/0022-3727/47/5/055110
90. Orlov D.A., Weigel U., Schwalm D., Terekhov A.S., Wolf A. Ultra-cold electron source with a GaAs-photocathode. Nuclear Instruments and Methods in Physics Research Section A: *Accelerators, Spectrometers, Detectors and Associated Equipment*, 2004, **Vol. 532(1–2)**, p. 418-421. DOI: 10.1016/j.nima.2004.06.048
91. Aliev A.Sh., Alekperov A.I., Pakhomov V.P., Fateev V.N. Photoelectrochemical behavior of gallium arsenide and the possibility of its protection against photocorrosion. *Electrochemistry*, 1985, **Vol. 21(3),** p. 370-372
92. Feng Ch., Liu J., Zhang Y., Qian Y., Song Y., Bao Y., Zhao . Comparison of photoemission performance of a GaAs photocathode between white light and monochromatic light illumination during activation. *Applied Optics*, 2019, **Vol. 58(32),** p. 8751-8756. DOI: 10.1364/AO.58.008751
93. Zhou R., Jani H., Zhang Y., Qian Y., Duan L. Photoelectron transportation dynamics in GaAs photocathodes. *J. Appl. Phys.* 2021, **Vol. 130**, 113101. DOI: 10.1063/5.0057458
94. Yamamoto N., Nakanishi T., Mano A., Nakagawa Y., Okumi Sh., Yamamoto M., Konomi T., Jin X., Ujihara T., Takeda Y., Ohshima T., Saka T., Kato T., Horinaka H., Yasue T., Koshikawa T., Kuwahara M. High brightness and high polarization electron source using transmission photocathode with GaAs-GaAsP superlattice layers. *J. Appl. Phys.* 2008, **Vol. 103**, 064905. DOI: 10.1063/1.2887930
95. Drouhin H.-J., Hermann C., Lampel G. Photoemission from activated gallium arsenide. I. Very-high-resolution energy distribution curves. *Phys. Rev. B,* 1985, **Vol. 31,** 3859. DOI: 10.1103/PhysRevB.31.3859
96. Zou J., Chang B., Yang Z., Zhang Y., Qiao J. Evolution of surface potential barrier for negative-electron-affinity GaAs photocathodes. *J. Appl. Phys.* 2009, **Vol. 105**, 013714. DOI: 10.1063/1.3063686
97. Zou J., Chang B., Yang Z., Qiao J., Zeng Y. Stability and photoemission characteristics for GaAs photocathodes in a demountable vacuum system. *Appl. Phys.*

Lett. 2008, **Vol. 92**, 172102. DOI: 10.1063/1.2918444
98. Zou J., Chang B., Chen H., Liu L. Variation of quantum-yield curves for GaAs photocathodes under illumination. *J. Appl. Phys.* 2007, **Vol. 101**, 033126. DOI: 10.1063/1.2435075
99. Liu Z., Sun Y., Peterson S., Pianetta P. Photoemission study of Cs–NF_3 activated GaAs(100) negative electron affinity photocathodes. *Appl. Phys. Lett.* 2008, **Vol. 92**, 241107. DOI: 10.1063/1.2945276
100. Yamamoto N., Yamamoto M., Kuwahara M., Sakai R., Morino T., Tamagaki K., Mano A., Utsu A., Okumi S., Nakanishi T., Kuriki M., Bo Ch., Ujihara T., Takeda Y. Thermal emittance measurements for electron beams produced from bulk and superlattice negative electron affinity photocathodes. *J. Appl. Phys.* 2007, **Vol. 102**, 024904. DOI: 10.1063/1.2756376
101. Orlov D.A., Krantz C., Wolf A., Jaroshevich A.S., Kosolobov S.N., Scheibler H.E., Terekhov A.S. Long term operation of high quantum efficiency GaAs(Cs,O) photocathodes using multiple recleaning by atomic hydrogen. *J. Appl. Phys.* 2009, **Vol. 106**, 054907. DOI: 10.1063/1.3208054
102. Zou J., Chang B., Yang Z., Zhang Y., Qiao J. Evolution of surface potential barrier for negative-electron-affinity GaAs photocathodes. *J. Appl. Phys.* 2009, **Vol. 105**, 013714. DOI: 10.1063/1.3063686
103. Pierce D.T., Meier F. Photoemission of spin-polarized electrons from GaAs. *Phys. Rev. B*, 1976, **Vol. 13**, 5484. DOI: 10.1103/PhysRevB.13.5484
104. Zhang Y., Niu J., Zhao J., Zou J., Chang B., Shi F., Cheng H. Influence of exponential-doping structure on photoemission capability of transmission-mode GaAs photocathodes. *J. Appl. Phys.* 2010, **Vol. 108**, 093108. DOI: 10.1063/1.3504193
105. Aulenbacher K., Schuler J., Harrach D.V., Reichert E., Röthgen J., Subashev A., Tioukine V., Yashin Y. Pulse response of thin III/V semiconductor photocathodes. *J. Appl. Phys.* 2002, **Vol. 92**, p. 7536–7543. DOI: 10.1063/1.1521526
106. Maruyama T., Luh D.-A., Brachmann A., Clendenin J.E., Garwin E.L., Harvey S., Kirby R.E., Prescott C.Y., Prepost R. Atomic hydrogen cleaning of polarized GaAs photocathodes. *Appl. Phys. Lett.* 2003, **Vol. 82**, p. 4184–4186. DOI: 10.1063/1.1581981
107. Sinclair C.K., Adderley P.A., Dunham B.M., Hansknecht J.C., Hartmann P., Poelker M., Price J.S., Rutt P.M., Schneider W.J. Development of a high average current polarized electron source with long cathode operational lifetime. *Phys. Rev. ST Accel. Beams*, 2007, **Vol. 10**, 023501. DOI: 10.1103/PhysRevSTAB.10.023501
108. Pastuszka S., Hoppe M., Kratzmann D., Schwalm D., Wolf A., Jaroshevich A.S., Kosolobov S.N., Orlov D.A., Terekhov A.S. Preparation and performance of transmission-mode GaAs photocathodes as sources for cold dc electron beams. *J. Appl. Phys.* 2000, **Vol. 88**, p. 6788–6800. DOI: 10.1063/1.1311307
109. Calabrese R., Guidi V., Lenisa P., Maciga B., Ciullo G., Della Mea G., Egeni G.P., Lamanna G., Rigato V., Rudello V., Yang B., Zandolin S., Tecchio L. Surface analysis of a GaAs electron source using Rutherford backscattering spectroscopy. *Appl. Phys. Lett.* 1994, **Vol. 65,** p. 301–302. DOI: 10.1063/1.112353
110. Alley R., Aoyagi H., Clendenin J., Frisch J., Garden C., Hoyt E., Kirby R., Klaisner L., Kulikov A., Miller R., Mulhollan G., Prescott C., Sáez P., Schultz D., Tang H., Turner J., Witte K., Woods M., Yeremian A.D., Zolotorev M. The Stanford linear accelerator polarized electron source. Nuclear Instruments and Methods in Physics Research Section A: *Accelerators, Spectrometers, Detectors and Associated Equipment*, 1995, **Vol. 365(1)**, p. 1-27. DOI: 10.1016/0168-9002(95)00450-5
111. Aulenbacher K., Nachtigall Ch., Andresen H.G., Bermuth J., Dombo Th., Drescher P., Euteneuer H., Fischer H., Harrach D.v., Hartmann P., Hoffmann J., Jennewein P., Kaiser K.H., Köbis S., Kreidel H.J., Langbein J., Petri

M., Plützer S., Reichert E., Schemies M., Schöpe H.-J., Steffens K.-H., .Steigerwald M., Trautner H., Weis Th. The MAMI source of polarized electrons. Nuclear Instruments and Methods in Physics Research Section A: *Accelerators, Spectrometers, Detectors and Associated Equipment*, 1997, **Vol. 391(3)**, p. 498-506.

112. Cates G.D., Hughes V.W., Michaels R., Schaefer H.R., Gay T.J., Lubell M.S., Wilson R., Dodson G.W., Dow K.A., Kowalski S.B., Isakovich K., Kumar K.S., Schulze M.E., Souder P.A., Kim D.H. The bates polarized electron source. Nuclear Instruments and Methods in Physics Research Section A: *Accelerators, Spectrometers, Detectors and Associated Equipment*, 1989, **Vol. 278(2)**, p. 293-317
113. Durek D., Frommberger F., Reichelt T., Westermann M. Degradation of a gallium-arsenide photoemitting NEA surface by water vapour. *Applied Surface Science*, 1999, **Vol. 143(1–4)**, p. 319-322. DOI: 10.1016/S0169-4332(99)00085-9
114. Pastuszka S., Terekhov A.S., Wolf A. 'Stable to unstable' transition in the (Cs, O) activation layer on GaAs (100) surfaces with negative electron affinity in extremely high vacuum. *Applied Surface Science*, 1996, **Vol. 99(4),** p. 361-365.
115. Sen P., Pickard D.S., Schneider J.E., McCord M.A., Pease R.F., Baum A.W., Costello K.A. Lifetime and reliability results for a negative electron affinity photocathode in a demountable vacuum system. *J. Vac. Sci. Technol. B,* 1998, **Vol. 16**, p. 3380–3384. DOI: 10.1116/1.590463
116. Sun Y., Kirby R.E., Maruyama T., Mulhollan G.A., Bierman J.C., Pianetta P. The surface activation layer of GaAs negative electron affinity photocathode activated by Cs, Li, and NF_3. *Appl. Phys. Lett.* 2009, **Vol. 95**, 174109. DOI: 10.1063/1.3257730
117. Malizia M., Seger B., Chorkendorff I., Vesborg P.C.K. Formation of a p–n heterojunction on GaP photocathodes for H_2 production providing an open-circuit voltage of 710 mV. *J. Mater. Chem. A*, 2014, **Vol. 2**, p. 6847-6853. DOI: 10.1039/C4TA00752B
118. Chitambar M., Wang Z., Liu Y., Rockett A., Maldonado S. Dye-Sensitized Photocathodes: Efficient Light-Stimulated Hole Injection into p-GaP Under Depletion Conditions. *Journal of the American Chemical Society,* 2012, **Vol. 134(25)**, p. 10670–10681. DOI:10.1021/ja304019n
119. Gutierrez W.A., Wilson H.L., Yee E.M. GaAs transmission photocathode grown by hybrid epitaxy. *Appl. Phys. Lett.* 1974, **Vol. 25**, p. 482–483. DOI: 10.1063/1.1655557
120. Aliyev A.Sh. Electrodeposition of thin CdS layers from a sulfuric acid electrolyte. *Azerb. Chem. Journal*. 2005, **no. 3**, p. 156-160
121. Aliev A.Sh., Mamedov M.N., Gulakhmedova Z.F., Abdulleva M.N. Preparation of thin electrolytic layers of CdS from sulfuric acid electrolyte. *Azerbaijan. Texniki Universiteti Elmi əsərlər "Fundamental elmlər"*, 2006, **Vol. 17(1)**, p. 122-124.
122. Aliyev A.Sh., Mamedov M.N., Babaeva M.A., Huseynzade T.L., Gulakhmedova Z.F. Mathematical description of the process of obtaining thin layers of cadmium-sulfur alloy from sulfuric acid electrolyte. *Chemical Problems*, 2006, **no. 3**, p. 522-524.
123. El-Rouby M., Aliev A.Sh., Gasanov Ch.A., Mamedov M.N. Electrodeposition of cadmium sulfide. *Inorganic materials*, 2012, **Vol. 48(2),** p. 194-206
124. Mammadov M.N., Алиев А.Ш., Elrouby M. Eletrodeposition of Cadmium Sulfide. *Thin Films Science and Technology*, 2012, **Vol.1(2),** p. 43-53
125. El-rouby M., Aliyev A.Sh. Electrochemical Synthesis of CdS on multi Walled Carbon Nanotubes Paste Electrode. *Advanced Materials Research*, 2013, **Vol. 787**, p. 417-422
126. El-rouby M., Aliyev A.Sh. Electrochemical Studies on the Cathodic Electrodeposition of n-type semiconductor CdS thin films from Thiosulfate Acidic Aqueous Solution. *Thin Films Science and Technology*, 2013, **Vol. 2(3)**, p. 195-205
127. El-rouby M., Aliyev A.Sh. Electrical, electrochemical and Photo-electrochemical studies on the electrodeposited n-type semiconductor

hexagonal crystalline CdS thin Film on nickel substrate. *Journal of Materials Science: Materials in Electronics*, 2014, **Vol. 25(12)**, p. 5618-5629

128. Aliyev A.Sh., Eminov Sh.O., Soltanova N.Sh., Majidzade V.A., Guliyev J.A., Jalilova Kh.D., Tagiyev D.B. Electrochemical production of thin films Cadmium Sulphide on nickel electrodes and research of their morphology. *Chemical Problems*, 2016, **Vol. 14(2),** p. 139-146
129. Eminov Sh.O., Aliyev A.Sh., Tagiyev D.B., Soltanova N.Sh., Guliyev J.A., Jalilova Kh.D., Ismayilov N.J., Hasanov I.S., Rajabli A .A., Mamedova G.Kh., Gurbanov I.I., Elrouby M. Photo and electrical peculiarities of the nanostructured glass /ITO/AAO and glass/ ITO/CdS systems. *Journal of Materials Science: Materials in Electronics*, 2016, **Vol. 27(9)**, p. 9853–9860. DOI: 10.1007/s10854-016-5053-9
130. Majidzade V.A., Soltanova N.Sh., Tagiyev D.B., Aliyev A.Sh., Fateev V.N. Some features of electrochemically deposited CdS nanowires. *Chemical Problems*, 2018, **Vol. 16(2)**, p. 178-185. DOI: 10.32737/2221-8688-2018-2-178-185
131. Eminov Sh.O., Aliyev A.Sh., Tagiyev D.B., Jalilova Kh.D., Guliyev J.A., Rajabli A.A., Mamedova G.H., Karimova A.Kh., Abdullayeva S.H., Majidzade V.A. Integration of supercarpacitor with solar cell based on NiO_2 and CdS nanopillars embedded in porous anodic alumina templates. *International Journal of Energy Research*, 2022, **Vol. 46**, p. 22134-22144. DOI: 10.1002/er.8741
132. Zhao E., Shan J., Yin P., Wang W., Du K., Yang Ch.-Ch., Guo J., Mao J., Peng Z., Wang C.-H., Ling T. Breaking Oxygen Evolution Limits on Metal Chalcogenide Photocatalysts for Visible-Light-Driven Overall Water-Splitting. *ACS Catal*. 2024, **Vol. 14(19)**, p. 14711–14720. DOI: 10.1021/acscatal.4c04444
133. Liu R., Zheng Z., Spurgeon J., Yang X. Enhanced photoelectrochemical water-splitting performance of semiconductors by surface passivation layers. *Energy Environ. Sci.*, 2014, **Vol. 7**, p. 2504-2517. DOI: 10.1039/C4EE00450G
134. Aliev A.S., Mamedov M.N., Abbasov M.T. Photoelectrochemical properties of TiO_2/CdS heterostructures. *Inorg Mater.,* 2009, **Vol. 45(9)**, p. 965–967. DOI: 10.1134/S0020168509090039
135. Pareek A., Paik P., Borse P.H. Nanoniobia Modification of CdS Photoanode for an Efficient and Stable Photoelectrochemical Cell. *Langmuir*, 2014, **Vol. 30(51)**, p. 15540–15549. DOI: 10.1021/la503713t
136. Khan M.M., Rahman A. Chalcogenides and Chalcogenide-Based Heterostructures as Photocatalysts for Water Splitting. *Catalysts*, 2022, **Vol. 12**, 1338. DOI: 10.3390/catal12111338
137. Ai G., Li H., Liu Sh., Mo R., Zhong J. Solar Water Splitting by TiO_2/CdS/Co–Pi Nanowire Array Photoanode Enhanced with Co–Pi as Hole Transfer Relay and CdS as Light Absorber. *Advanced Functional Materials*, 2015, **Vol. 25(35),** p. 5706-5713. DOI: 10.1002/adfm.201502461
138. Mammadon M.N., Aliyev A.Sh. Some electrical properties of cadmium-tellurium electrolytic alloys. *Chemical Problems*, 2003, **no. 3**, p. 63-65.
139. Mammadov M.N., Aliyev A.Sh., Babayeva M.A., Abbasova Z.A., Huseynova R.A., Ganbarova N.A. Photoelectrochemical properties of the CdTe/TiO_2 heterosystem. *Azerb. Chem. Journal*, 2005, **no. 1**, p. 127–129
140. Aliev A.Sh. Electrochemical production of thin layers of Cd–Te alloys from a fluorine-borate electrolyte. *Chemical Problems*, 2005, **no. 1**, p. 20-22
141. Aliyev A.Sh. Electrodeposition of thin CdTe films. *Bulletin AN Georgia. Ser. Chemical*, 2005, **no. 3-4**, p. 307–312
142. Aliyev A.Sh. Electrodeposition of thin films of CdTe cadmium chalcogenides. *Azerb. Chem. Journal*, 2006, **no. 2**, p. 46–52
143. Aliyev A.Sh. Electrodeposition of thin films of cadmium chalcogenides. *Azerb. Chem. Journal*, 2006, **no. 3**, p. 103–113
144. Mamedov M.N., Aliev A.Sh. Electrical properties of electrodeposited CdTe thin

films. *Inorg Mater.* **44**, 2008, p. 804–806. DOI:10.1134/S0020168508080049.
145. Lichterman M.F., Carim A.I., McDowell M.T., Hu Sh., Gray H.B., Brunschwig B.S., Lewis N.S. Stabilization of n-cadmium telluride photoanodes for water oxidation to O_2(g) in aqueous alkaline electrolytes using amorphous TiO_2 films formed by atomic-layer deposition. *Energy Environ. Sci.*, 2014, **Vol. 7**, p. 3334-3337. DOI: 10.1039/C4EE01914H
146. Aliyev A.Sh., Mammadov M.N. Electrodeposition of thin CdSe layers on a Pt electrode. *Chemistry and chemical technology*, 2007, **Vol. 50(12),** c. 70-73
147. Aliyev A.Sh. Electrical properties of thin electrolytic layers of CdSe. *Chemical Problems*, 2008, **no. 12**, p. 394-395
148. Aliyev A.Sh., Mammadov M.N. Photoelectrochemical behavior of the CdSe/WO_3 semiconductor heterosystem. *Chemistry and chemical technology*, 2009, **Vol. 52(4)**, p. 61-63
149. Aliev A.Sh., Mamedov M.N. Electrodeposition of thin CdSe films from a sulfuric acid electrolyte. *St. Petersburg University Bulletin. Series: Physics and Chemistry*, 2009, **Vol. 4(1),** p. 115–121
150. Aliev A.Sh., Mamedov M.N., Abbasov M.T. Deposition of thin electroplated Cd-Se layers. *Russ J Appl Chem.* 2009, **Vol. 82**, p. 1022–1024. DOI:10.1134/S1070427209060172
151. Mamedov M.N., Aliyev A.Sh., Huseynova R.G. X-ray phase analysis of thin electrolytic layers of Cd–Te and Cd–Se. *Chemical Problems*, 2009, **no. 4**, p. 664–667
152. Wang G., Li Y. Nickel Catalyst Boosts Solar Hydrogen Generation of CdSe Nanocrystals. *ChemCatChem*, 2013, **Vol. 5(6),** p. 1294-1295. DOI: 10.1002/cctc.201300034
153. Abdullayev N.M., Ibrahimova L.N., Aliyev M.E., Aliyev Y.I. Investigation of the atomic dynamics of CdSe thin layers by raman spectroscopy. *Chemical Problems*, 2024, **Vol. 22(2)**, p. 231–236. DOI: 10.32737/2221-8688-2024-2-231-236
154. Buharov P.V. Photocathodes of modern image intensifier. Reports from Tomsk State University of Control Systems and Radioelectronics. 2011, **Vol. 24(2),** p. 106-109
155. Moniz S.J.A., Shevlin S.A., Martin D.J., Guo Z.-X., Tang J. Visible-light driven heterojunction photocatalysts for water splitting – a critical review. *Energy Environ. Sci.*, 2015, **Vol. 8**, p. 731-759. DOI: 10.1039/C4EE03271C
156. Paracchino A., Mathews N., Hisatomi T., Stefik M., Tilley S.D., Grätzel M. Ultrathin films on copper(I) oxidewater splitting photocathodes: a study on performance and stability. *Energy Environ. Sci.*, 2012, **Vol. 5**, p. 8673-8681. DOI: 10.1039/C2EE22063F
157. Genaro-Saldivar K.F., Negrete-Reyes G.R., Ramirez-Meneses E., Juarez-Balderas C., Avendano-Sanjuan F., Garcia-Najera D.A., Ibanez J.G. Simultaneous anodic and cathodic electrodeposition of Cu_2O for solar energy conversion. *Chemical Problems*, 2024, **Vol. 22(4)**, p. 447–457. DOI: 10.32737/2221-8688-2024-4-447-457
158. Bagal I.V., Chodankar N.R., Hassan M.A ., Waseem A., Johar M.A., Kim D.-H., Ryu S.-W. Cu_2O as an emerging photocathode for solar water splitting - A status review. *International Journal of Hydrogen Energy*, 2019, **Vol. 44(39)**, p. 21351-21378. DOI: 10.1016/j.ijhydene.2019.06.184
159. Wang Y.-Ch., Qin Ch., Lou Z.-R., Lu Y., Zhu L.-P. Cu_2O photocathodes for unassisted solar water-splitting devices enabled by noble-metal cocatalysts simultaneously as hydrogen evolution catalysts and protection layers. *Nanotechnology*, 2019, **Vol. 30(9),** 5407, DOI: 10.1088/1361-6528/ab40e8
160. Son M.-K. Key Strategies on Cu_2O Photocathodes toward Practical Photoelectrochemical Water Splitting. *Nanomaterials,* 2023, **Vol. 13(24)**, 3142. DOI: 10.3390/nano13243142
161. Dubale A.A., Su W.-N., Tamirat A.G., Pan Ch.-J., Aragaw B.A., Chen H.-M., Chen C.-H., Hwang B.-J. The synergetic effect of graphene on Cu_2O nanowire arrays as a highly efficient hydrogen evolution photocathode in water splitting. *J. Mater. Chem. A*, 2014,

Vol. 2, p. 18383-18397. DOI: 10.1039/C4TA03464C

162. Jung K., Lim T., Bae H., Ha J.-S., Martinez-Morales A.A. Cu_2O Photocathode with Faster Charge Transfer by Fully Reacted Cu Seed Layer to Enhance Performance of Hydrogen Evolution in Solar Water Splitting Applications. *ChemCatChem*, 2019, **Vol. 11**, p. 4377–4382. DOI: 10.1002/cctc.201900526
163. Jian J., Kumar R., Sun J. Cu_2O/ZnO p−n Junction Decorated with NiO_x as a Protective Layer and Cocatalyst for Enhanced Photoelectrochemical Water Splitting. *ACS Appl. Energy Mater*. 2020, **Vol. 3**, p. 10408−10414. DOI: 10.1021/acsaem.0c01198
164. Wang Y.-Ch., Qin Ch., Lou Z.-R., Lu Y.-F., Zhu L.-P. Cu_2O photocathodes for unassisted solar water-splitting devices enabled by noble-metal cocatalysts simultaneously as hydrogen evolution catalysts and protection layers. *Nanotechnology*, 2019, **Vol. 30(49)**, 495407. DOI: 10.1088/1361-6528/ab40e8.
165. Yadav N., Pant K.K., Tripathi K., Yadav G., Ahmaruzzaman M d. Harnessing metal sulfides for efficient hydrogen production employing photocatalytic water splitting: Current status and future direction. *International Journal of Hydrogen Energy*, 2025, **Vol. 101**, p. 1221-1253. DOI: 10.1016/j.ijhydene.2024.12.516
166. Sun L., Zhao Z., Li Sh., Su Y., Huang L., Shao N., Liu F., Bu Y., Zhang H., Zhang Z. Role of SnS_2 in 2D–2D SnS_2/TiO_2 Nanosheet Heterojunctions for Photocatalytic Hydrogen Evolution. *ACS Appl. Nano Mater*. 2019, **Vol. 2(4)**, p. 2144–2151. DOI:10.1021/acsanm.9b00122
167. Pareek A., Borse P.H. Hurdles and recent developments for CdS and chalcogenide-based electrode in “Solar electro catalytic” hydrogen generation: A review. *Electrochemical Science Advances*, 2022, **Vol. 2(6)**, e2100114. DOI: 10.1002/elsa.202100114
168. Chanda N., Mehmood S., Abraham B.M., Bojja S., Pal U. Charge-Transfer Modulation on CdS Artificial Leaf for Efficient Hydrogen Generation. *ACS Appl. Nano Mater*. 2024, **Vol. 7(7)**, p. 6861–6872. DOI: 10.1021/acsanm.3c05636
169. Alfa I., Hafeez H.Y., Mohammed J., Abdu S., Suleiman A.B., Ndikilar C.E. A recent progress and advancement on MoS_2-based photocatalysts for efficient solar fuel (hydrogen) generation *via* photocatalytic water splitting. *International Journal of Hydrogen Energy*, 2024, Vol. 71, p. 1006-1025. DOI: 10.1016/j.ijhydene.2024.05.203
170. Hasani A., Le Q.V., Tekalgne M., Choi M.-J., Lee T.H., Jang H.W., Kim S.Y. Direct synthesis of two-dimensional MoS_2 on *p*-type Si and application to solar hydrogen production. *NPG Asia Mater*. 2019, **Vol. 11**, 47. DOI: 10.1038/s41427-019-0145-7
171. Obodo P.Ch., Obodo K.O., Aigbe U.O., Aigbodion V. Recent Advances in Molybdenum Disulfide (MoS_2) and MXene-based Heterostructures for Photovoltaic and Water Splitting Applications: A Review. *ChemistrySelect*, 2025, Vol. 10(15), e202404995. DOI: 10.1002/slct.202404995
172. Xie Z., Yu Sh., Ma X., Li K., Ding L., Wang W., Cullen D.A., Meyer III H.M., Yu H., Ton g J., Wu Z., Zhang F.-Y. MoS_2 nanosheet integrated electrodes with engineered 1T-2H phases and defects for efficient hydrogen production in practical PEM electrolysis. *Applied Catalysis B: Environmental*, 2022, **Vol. 313**, 121458. DOI: 10.1016/j.apcatb.2022.121458
173. Ding X., Liu D., Zhao P., Chen X., Wang H., Oropeza F.E., Gorni G., Barawi M., García-Tecedor M., de la Peña O’Shea V.A., Hofmann J.P., Li J., Kim J., Cho S., Wu R., Zhang K.H.L. Dynamic restructuring of nickel sulfides for electrocatalytic hydrogen evolution reaction. *Nature Communications*, 2024, **Vol. 15,** 5336. DOI:10.1038/s41467-024-49015-4
174. Pang H., Wei Ch., Li X., Li G., Ma Y., Li S., Chen J., Zhang J. Microwave-assisted synthesis of NiS_2 nanostructures for

supercapacitors and cocatalytic enhancing photocatalytic H_2 production. *Scientific Reports*, 2014, **Vol. 4**, 3577. DOI: 10.1038/srep03577

175. Ma Q., Hu Ch., Liu K., Hung S.F., Ou D., Chen H.M., Fu G., Zheng N. Identifying the electrocatalytic sites of nickel disulfide in alkaline hydrogen evolution reaction. *Nano Energy*, 2017, **Vol. 41**, p. 148-153
176. Thiehmed Z., Shakoor A., Altahtamouni T. Recent Advances in WS_2 and Its Based Heterostructures for Water-Splitting Applications. *Catalysts*, 2021, **Vol. 11**, 1283. DOI: 10.3390/catal11111283
177. Ghanghass A., Bhatia R. Optimized hydrothermal transformation of WO_3 nanorods into WS_2 based catalysts: enhanced hydrogen evolution performance and synergistic effects with CNT. *Phys. Scr.,* 2025, **Vol. 100(4),** 045915. DOI: 10.1088/1402-4896/adb2c2
178. Wu L., van Hoof A.J. F., Dzade N.Y., Gao L., Richard M.-I., Friedrich H., de Leeuw N.H., Hensen E.J.M., Hofmann J.P. Enhancing the electrocatalytic activity of 2H-WS_2 for hydrogen evolution via defect engineering. *Physical Chemistry Chemical Physics*, 2019, **Vol. 21(11),** p. 6071-6079. DOI: 10.1039/c9cp00722a
179. Shuklova I.A., Razumov V.F. Lead chalcogenide quantum dots for photoelectric devices. *Russ. Chem. Rev*., 2020, **Vol. 89(3)**, p. 379-391. DOI:10.1070/RCR4917
180. Matoba K., Takahashi M., Matsuda Y., Higashimoto Sh. Photoelectrochemical water splitting on the Pt-In_2S_3/$CuInS_2$ photoelectrode under solar light irradiation: Effects of electrolytes on the solar energy to hydrogen conversion. *Journal of Electroanalytical Chemistry*, 2021, **Vol. 895**, 115489. DOI:10.1016/j.jelechem.2021.115489
181. Le Donne A., Trifiletti V., Binetti S. New Earth-Abundant Thin Film Solar Cells Based on Chalcogenides. *Frontiers in Chemistry*, 2019, **Vol. 7**, 297. DOI: 10.3389/fchem.2019.00297
182. Kiptarus J.J., Korir K.K., Githinji D.N., Kiriamiti H.K. Improved photocatalytic performance of cobalt doped ZnS decorated with graphene nanostructures under ultraviolet and visible light for efficient hydrogen production. *Scientific Reports*, 2024, **Vol. 14**, 21632. DOI:10.1038/s41598-024-72645-z
183. Vamvasakis I., Andreou E.K., Armatas G.S. Mesoporous Dual-Semiconductor ZnS/CdS Nanocomposites as Efficient Visible Light Photocatalysts for Hydrogen Generation. *Nanomaterials (Basel)*, 2023, **Vol. 13(17)**, 2426. DOI: 10.3390/nano13172426
184. Chatterjee A., Kiran Kumar G., Roymahapatra G., Das H.S., Jaishree G., Siva Rao T. Zinc chalcogenide nanostructures: synthesis methodologies and applications—a review. *Front. Nanotechnol*., *Sec. Nanomaterials* 2024, **Vol. 6**, DOI:10.3389/fnano.2024.1433591
185. Sahu R., Jain S.K., Tripathi B. Multi-walled carbon nanotubes (MWCNTs) dispersed ZnS based photocatalytic activity for solar hydrogen production. *J. Nano- Electron. Phys*. 2021, **Vol.13(1,)** 01027. DOI: 10.21272/jnep.13(1).01027
186. Mendoza C.-G., Rodríguez Arias J.I., Morales-Mendoza G., Oros-Ruiz S., Garcia-Zaleta D., Frías Márquez D.M. García R.L., López-González R. Optimization of ZnS synthesis through the incorporation of monoethanolamine (MEA) for the efficient photocatalytic production of H_2. *Journal of Materials Science: Materials in Engineering*, 2025, **Vol. 20**, 50. DOI: 10.1186/s40712-025-00261-4
187. Shinoda K., Arai T., Ohshima H., Jeyadevan B., Muramatsu A., Tohji K., Matsubara E. Local Atomic Structure and Electronic State of ZnS Films Synthesized by Using CBD Technique. *Materials Transactions*, 2002, **Vol. 43(7),** p. 1512 – 1516.
188. Ahmad H., Kamarudin S.K., Minggu L.J., Kassim M. Hydrogen from photo-catalytic water splitting process: a review. *Renew Sustain Energy Rev*, 2015, **Vol. 43**, p. 599-610. DOI:10.1016/J.RSER.2014.10.101
189. Rao V.N., Ravi P., Sathish M., Vijayakumar M., Sakar M., Karthik M., Balakumar S., Reddy K.R., Shetti N.P., Aminabhavi T.M., Shankar M.V. Metal

chalcogenide-based core/shell photocatalysts for solar hydrogen production: Recent advances, properties and technology challenges. *Journal of Hazardous Materials*, 2021, **Vol. 415**, 125588. DOI: 10.1016/j.jhazmat.2021.125588

190. Zhu Sh.-Ch., Xiao F.-X. Transition Metal Chalcogenides Quantum Dots: Emerging Building Blocks toward Solar-to-Hydrogen Conversion. *ACS Catalysis,* 2023, **Vol. 13(11),** p. 7269–7309. DOI: 10.1021/acscatal.2c05401
191. Li J., Jiménez-Calvo P., Paineau E., Ghazzal M.N. Metal Chalcogenides Based Heterojunctions and Novel Nanostructures for Photocatalytic Hydrogen Evolution. *Catalysts,* 2020, **Vol. 10(1)**, 89. DOI: 10.3390/catal10010089
192. Alonso-Vante N. *Chalcogenide Materials for Energy Conversion. Nanostructure Science and Technology.* 2018. Springer International Publishing. 226 p. DOI: 10.1007/978-3-319-89612-0
193. Molaei M.J. Recent advances in hydrogen production through photocatalytic water splitting: a review. *Fuel*, 2024, **Vol. 365**, 131159. DOI: 10.1016/J.FUEL.2024.131159
194. Li S., Zhang L., Jiang T., Chen L., Lin Y., Wang D., Xie T. Construction of shallow surface states through light Ni doping for high-efficiency photocatalytic hydrogen production of CdS nanocrystals. *Chem. Eur. J*, 2014, **Vol. 20**, p. 311-316. DOI: 10.1002/chem.201302679
195. Shahid M.U., Najam T., Helal M.H., Hossain I., El-Bahy S.M., El-Bahy Z.M., ur Rehman A., Ahmad Shah S.Sh., Nazir M.A. Transition metal chalcogenides and phosphides for photocatalytic H_2 generation via water splitting: a critical review. *International Journal of Hydrogen Energy*, 2024, **Vol. 62**, p. 1113-1138. DOI:10.1016/j.ijhydene.2024.03.139
196. Wang J., Lin S., Tian N., Ma T., Zhang Y., Huang H. Nanostructured metal sulfides: classification, modification strategy, and solar-driven CO_2 reduction application. *Adv. Funct. Mater.*, 2021, **Vol. 31**, 2008008. DOI: 10.1002/ADFM.202008008
197. Shanmugaratnam S., Selvaratnam B., Baride A., Koodali R., Ravirajan P., Velauthapillai D., Shivatharsiny Y. SnS_2/TiO_2 Nanocomposites for Hydrogen Production and Photodegradation under Extended Solar Irradiation. *Catalysts,* 2021, **Vol. 11(5)**, 589. DOI: 10.3390/catal11050589
198. Mishra R.K., Choi G.J., Choi H.J., Singh J., Lee S.H., Gwag J.S. Potentialities of nanostructured SnS_2 for electrocatalytic water splitting: A review. *Journal of Alloys and Compounds*, 2022, **Vol. 921**, 166018. DOI: 10.1016/j.jallcom.2022.166018
199. Molina-Jiménez J.P., Horta-Piñeres S.D., Castillo S.J., Izquierdo J.L., Avila D.A. Ultra-Thin Films of CdS Doped with Silver: Synthesis and Modification of Optical, Structural, and Morphological Properties by the Doping Concentration Effect. *Coatings,* 2025, Vol. 15(4), 431. DOİ: 10.3390/coatings15040431
200. Jafarova S.F., Majidzade V.A., Kasimogli I., Eminov Sh.O., Aliyev A.Sh., Azizova A.N., Tagiyev D.B. Electrical and Photoelectrochemical Properties of Thin MoS_2 Films Produced by Electrodeposition. *Inorganic Materials*, 2021, **Vol. 57(4)**, p. 331-336. DOI:10.1134/S0020168521040105
201. Luo P., Zhang H., Liu L., Zhang Y., Deng J., Xu C., Hu N., Wang Y. Целенаправленный синтез уникальных микроархитектур сульфида никеля (NiS, NiS_2) и их применение в усовершенствованных системах расщепления воды. *ACS Appl. Mater. Interfaces,* 2017, **Vol. 9**, p. 2500–2508. DOI: 10.1021/acsami.6b13984
202. Majidzade V.A., Mammadova S.P., Petkucheva E.S., Slavcheva E.P., Aliyev A.Sh. Tagiyev D.B. Co-electrodeposition of iron and sulfur in aqueous and non-aqueous electrolytes. *Bulgarian Chemical Communications*, 2020, **Vol. 52, Special Issue E**, p. 73-78
203. Kadam S.A., Jaihindh D.P., Chen Y.-R., Kadam K.P., Hsieh H.-W., Bera S.,

Santosh K.C., Sumant A.V., Fu Y.-P., Lai Ch.-Ch., Ma Y.-R., Pradhan N.R. Ferromagnetic Hybrid 2D FeS/FeS_2 Nanostructures as Electrocatalysts for the Hydrogen Evolution Reaction. *ACS Applied Nano Materials,* 2024, **Vol. 7(23)**, p. 27566–27578. DOI: 10.1021/acsanm.4c05598

204. Yin L., Hai X., Chang K., Ichihara F., Ye J. Synergetic exfoliation and lateral size engineering of MoS_2 for enhanced photocatalytic hydrogen generation. *Small*, 2018, **Vol. 14(14)**, 1704153. DOI: 10.1002/smll.201704153
205. Ali Shah S., Khan I., Yuan A. MoS_2 as a co-catalyst for photocatalytic hydrogen production: a mini review. *Molecules*, 2022, **Vol. 27(10)**, 3289. DOI:10.3390/molecules27103289
206. Aleithan S.H., Laradhi Sh.S., Al-Amer K., Abd El-Lateef H.M. Synergistic MoS_2–Gold Nanohybrids for Sustainable Hydrogen Production. *Catalysts,* 2025, **Vol. 15(6),** 550. DOI: 10.3390/catal15060550
207. Friedrich D., Schlosser M., Pfitzner A. Interconversion of one-dimensional thiogallates $Cs_2[Ga_2(S_2)_{2-x}S_{2+x}](x= 0, 1, 2)$ by using high-temperature decomposition and polysulfide-flux reactions. *Cryst Growth Des*, 2017, **Vol. 17(9),** p. 4887-4892. DOI: 10.1021/acs.cgd.7b00840
208. Ouyang Ch., Quan X., Zhang Ch., Pan Y., Li X., Hong Zh., Zhi M. Direct Z-scheme $ZnIn_2S_4$@MoO_3 heterojunction for efficient photodegradation of tetracycline hydrochloride under visible light irradiation. *Chemical Engineering Journal*, 2021, **Vol. 424**, 130510. DOI: 10.1016/j.cej.2021.130510
209. Schoonman J.. Production of Hydrogen with Solar Energy. Handbook of Clean Energy Systems. 2015. p. 1–23. DOI:10.1002/9781118991978.hces006
210. Khan M.M. *Chalcogenide-based nanomaterials as photocatalysts*. Elsevier. 2021. 350 p. DOI: 10.1016/C2019-0-01819-5
211. Maurya O., Khaladkar S., Horn M.R., Sinha B., Deshmukh R., Wang H., Kim T.Y., Dubal D.P., Kalekar A. Emergence of Ni-Based Chalcogenides (S and Se) for Clean Energy Conversion and Storage. *Small*, 2021, **Vol. 17(33)**, e2100361. DOI: 10.1002/smll.202100361.
212. Sudeep M., Rajyaguru Y.V., Rastogi Ch. K., Sham Aan M.P., Sridharan M., Khosla A., Manj unatha C. Recent development of nickel based chalcogenides for hydrogen generation. *Materials Today: Proceedings*, 2023, **Vol. 73(2)**, p. 316-322. DOI: 10.1016/j.matpr.2022.10.244
213. Kim M., Joung S., Lee S., Kwon H., Lee H. Recent advances in Ni-based electrocatalysts for low-energy hydrogen production via alternative pathways to water electrolysis. *Energy Mater.* **2025**, **Vol. 5**, 500097. DOI: 10.20517/energymater.2024.244
214. Swesi A.T., Masud J., Liyanage W.P.R., Siddesh U., Bohannan E., Medvedeva J., Nath M. Textured $NiSe_2$ Film: Bifunctional Electrocatalyst for Full Water Splitting at Remarkably Low Overpotential with High Energy Efficiency. *Scientific Reports,* 2017, **Vol. 7**, 2401. DOI: 10.1038/s41598-017-02285-z
215. Pi Z.-G., Ye H., Han Z., Yu P., Yin Z., Ma X. Promising $CoSe_2$-CNT composite catalyst for efficient photoelectrochemical hydrogen evolution reaction. *Frontiers in Materials*, 2022, **Vol. 9**, 1005221. DOI: 10.3389/fmats.2022.1005221
216. Chen Ch.-J., Yang K.-Ch., Basu M., Lu T.-H., Lu Y.-R., Dong C.-L., Hu S.-F., Liu R.-S. Wide Range pH-Tolerable Silicon@Pyrite Cobalt Dichalcogenide Microwire Array Photoelectrodes for Solar Hydrogen Evolution. *ACS Appl. Mater. Interfaces,* 2016, **Vol. 8(8)**, p. 5400–5407. DOI:10.1021/acsami.6b00027
217. Zhou J., Cheng Y., Zhu Y. Survey of Tetragonal Transition Metal Chalcogenide Hetero-Bilayers for Promising Photocatalysts. *Advanced Materials Interfaces*, 2022, **Vol. 9(10)**, p. 2102334. DOI: 10.1002/admi.202102334
218. Wang Y., Han Y., Zhao R., Han J., Wang L. Efficient flower-like ZnSe/$Cu_{0.08}Zn_{0.92}S$ photocatalyst for hydrogen production application. *Front. Chem. Sci. Eng.* 2023,

Vol. 17, p. 1301–1310. DOI: 10.1007/s11705-022-2295-3

219. Sun Y., Sun Z., Gao S., Cheng H., Liu Q., Piao J., Yao Tao, Wu Ch., Hu S., Wei S., Xie Y. Fabrication of flexible and freestanding zinc chalcogenide single layers. *Nature Communications,* 2012, **Vol. 3**, 1057. DOI: 10.1038/ncomms2066
220. Nworie I.C., Ishiwu S.M.U., Agbo P.E., Ojobeagu A.O., Otah P.B., Mbamara C., Ojobo B. Comparative Assessment of Optical and Solid-State Characteristics in Antimony-Doped Chalcogenide Thin Films of ZnSe and PbSe to Boost Photovoltaic Performance in Solar Cells. *Nigerian Journal of Physics*, 2024, Vol. 33(1), p. 16-22. DOI: 10.62292/njp.v33i1.2024.202
221. Majidzade V.A., Javadova S.P., Jafarova S.F., Mirzayeva A.M., Aliyev A.Sh. Investigation of electrocatalytic properties of electrodeposited Sb_2Se_3 thin films in neutral medium. *Azerbaijan Chemical Journal*, 2025, **no. 2**, p. 79-87. DOI: 10.32737/0005-2531-2025-2-79-87
222. Majidzade V.A., Aliyev A.Sh., Guliyev P.H., Babanly D.M. Electrodeposition of the Sb_2Se_3 thin films on various substrates from the tartaric electrolyte. *Electrochemical Science and Engineering*, 2020, **Vol. 10(1),** p. 1-9. DOI: 10.5599/jese.676
223. Majidzade V.A., Javadova S.P., Aliyev G.S., Aliyev A.Sh., Tagiyev D.B. Electrodeposition of Sb–Se Thin Films from Organic Electrolyte. *Chemistry Africa*, 2022, **Vol. 5(6),** p. 2085-2094. DOI: 10.1007/s42250-022-00480-8
224. Majidzade V.A. Sb_2Se_3-based solar cells: obtaining and properties. *Chemical Problems*, 2020, **Vol. 18(2),** p. 181-198. DOI: 10.32737/2221-8688-2020-2-181-198
225. Majidzade V.A., Aliyev A.Sh., Qasimogli İ., Quliyev P.H., Tagiyev D.B. Electrical properties of electrochemically grown thin Sb_2Se_3 semiconductor films. *Inorganic Materials*, 2019, **Vol. 55(10),** p. 979–983. DOI: 10.1134/S0020168519100108
226. Majidzade V.A., Aliyev G.S., Javadova S.P., Aliyev A.Sh., Dadashova S.D., Tagiyev D.B. Mathematical modeling and optimization of the process of formation of functional thin $MoSe_2$ films. *Mathematical Models and Computer Simulations,* 2023, **Vol. 15(1)**, p. 73-78. DOI: 10.1134/S2070048223010118
227. Majidzade V.A., Jafarova S.F., Javadova S.P., Azizova A.N., Dadashova S.D., Aliyev A.Sh., Tagiyev D.B. Electrodeposıtıon of Mo-Se thın fılms and the ınfluence of the maın factors on theır composıtıon. *Bulgarian Chemical Communications*, 2025, **Vol. 57(2),** p. 102-107. DOI: 10.34049/bcc.57.2.5694
228. Ali Syed A., Ahmad T. Chemical strategies in molybdenum based chalcogenides nanostructures for photocatalysis. *International Journal of Hydrogen Energy*, 2022, **Vol. 47(68)**, p. 29255-29283. DOI: 10.1016/j.ijhydene.2022.06.269
229. Poorahong S., Izquierdo R., Siaj M. An efficient porous molybdenum diselenide catalyst for electrochemical hydrogen generation. *J. Mater. Chem. A*, 2017, **Vol. 5(39)**, p. 20993-21001. DOI: 10.1039/C7TA05826H
230. Bozheyev F., Harbauer K., Zahn C., Friedrich D., Ellmer K. Highly (001)-textured p-type WSe_2 Thin Films as Efficient Large-Area Photocathodes for Solar Hydrogen Evolution. *Sci Rep.,* 2017, **Vol. 7**, 16003. DOI: 10.1038/s41598-017-16283-8
231. Rubinkovskaya O.V., Fominski D.V., Nevolin V.N., Romanov R.I., Kartsev P.F., Jiang H., Fominski V.Yu. Thin Nanostructured n-WSe_2 Films and Their Application in Semiconductor p-Si Photocathodes for Hydrogen Production by Water Splitting. *Inorg. Mater. Appl. Res.,* 2023, **Vol. 14**, p. 1198–1206. DOI: 10.1134/S2075113323050404
232. Hussain S., Chae J., Akbar K., Vikraman D., Truong L., Naqvi B.A., Abbas Y., Kim H.-S., Chun S.-H., Kim G., Jung J. Fabrication of Robust Hydrogen Evolution Reaction Electrocatalyst Using Ag_2Se by Vacuum Evaporation. *Nanomaterials*, 2019, **Vol. 9(10),** 1460. DOI: 10.3390/nano9101460

233. Zeynalova A.O., Majidzade V.A., Javadova S.P., Aliyev A.Sh. Electrochemical synthesis of iron monoselenide thin films. *Chemical Problems*, 2021, **Vol. 19(4),** p. 262-271. DOI: 10.32737/2221-8688-2021-4-262-271
234. Haciyeva V.I., Babayev Sh.Z. Influence of gamma, electron, proton and gamma neutron ırradıatıon on photodıodes based on InSe wıth ımproved parameters. *Chemical Problems*, 2025, **Vol. 23(2),** p. 266-271. DOI: 10.32737/2221-8688-2025-2-266-271
235. Zhong W., Zhao B., Yu H., Fan J. Simultaneously Optimizing the Number and Efficiency of Active Se Sites in Se-Rich a-$MoSe_x$ Nanodot Cocatalysts for Efficient Photocatalytic H_2 Evolution. *Sol RRL*, 2022, **Vol. 6(1),** 2100832. DOI: 10.1002/solr.202100832
236. Tayyab M., Liu Y., Liu Z., Xu Z., Yue W., Zhou L., Lei J., Zhang J. A new breakthrough in photocatalytic hydrogen evolution by amorphous and chalcogenide enriched cocatalysts. *Chem. Eng. J.*, 2023, **Vol. 455**, 140601. DOI: 10.1016/j.cej.2022.140601
237. Yang Y., Zhang D., Xiang Q. Plasma-modified $Ti_3C_2T_x$/CdS hybrids with oxygen-containing groups for high-efficiency photocatalytic hydrogen production. *Nanoscale*, 2019, **Vol. 11(40)**, p. 18797-18805. DOI: 10.1039/c9nr07242j
238. Zhu Sh.-Ch., Wang Z.-Ch., Tang B., Liang H., Liu B.-J., Li Sh., Chen Z., Cheng N.-C., Xiao F.-X. Progressively stimulating carrier motion over transient metal chalcogenide quantum dots towards solar-to-hydrogen conversion. *J. Mater. Chem. A*, 2022, **Vol. 10**, p. 11926-11937. DOI: 10.1039/D2TA02755K
239. Gao D., Wu X., Wang P., Yu H., Zhu B., Fan J., Yu J. Selenium-enriched amorphous $NiSe_{1+x}$ nanoclusters as a highly efficient cocatalyst for photocatalytic H_2 evolution. *Chem. Eng. J.*, 2021, **Vol. 408**, 127230. DOI: 10.1016/j.cej.2020.127230
240. Deng Sh., Zhong Y., Zeng Y., Wang Y., Yao Zh., Yang F., Lin Sh., Wang X., Lu X., Xia X., Tu J. Directional construction of vertical nitrogen-doped 1T-2H $MoSe_2$/graphene shell/core nanoflake arrays for efficient hydrogen evolution reaction. *Adv. Mater.*, 2017, **Vol. 29(21),** 1700748. DOI: 10.1002/adma.201700748
241. Sun W., Liu Z., Liu D., Zhang B., Li Y., Wang Ch., Liu X., Wang X., Song X.-Z., Tan Z. $MoSe_2$ embedded in (NiCo)Se_2 nanosheets to form heterostructure materials for high stability supercapacitors and efficient hydrogen evolution. *J. Mater. Chem. A*, 2025, **Vol. 13(28)**, p. 22792-22803. DOI: 10.1039/D5TA02996A
242. Li Y., Wang Ch., Abdukayum A., Feng L. Advances in green hydrogen generation based on $MoSe_2$ hybrid catalysts. *Electrochimica Acta*, 2024, **Vol. 503,** 144891. DOI: 10.1016/j.electacta.2024.144891
243. Zhang T., Cai Y., Lou Y., Chen J. 1T-2H $MoSe_2$ modified $MAPbI_3$ for effective photocatalytic hydrogen evolution. *Journal of Alloys and Compounds*, 2022, **Vol. 893,** 162329. DOI: 10.1016/j.jallcom.2021.162329
244. Karunanithy M., Prabhavathi G., Hameedha B.A., Ibraheem B.H.A., Kaviyarasu K., Nivetha S., Punithavelan N., Ayeshamariam A., Jayachandran M. Nanostructured Metal Tellurides and Their Heterostructures for Thermoelectric Applications—A Review. *J. Nanosci. Nanotechnol.*, 2018, **Vol. 18(10)**, p. 6680-6707. DOI: 10.1166/jnn.2018.15731
245. Gao D., Zhong W., Liu Y., Yu H., Fan J. Synergism of tellurium-rich structure and amorphization of $NiTe_{1+x}$ nanodots for efficient photocatalytic H_2-evolution of TiO_2. *Appl. Catal. B Environ.*, 2021, **Vol. 290**, 120057. DOI: 10.1016/j.apcatb.2021.120057
246. Sharma R.K., Rastogi A.C., Singh G. Electrochemical growth and characterization of manganese telluride thin films. *Materials Chemistry and Physics*, 2004, **Vol. 84(1)**, p. 46-51. DOI: 10.1016/j.matchemphys.2003.09.052

247. Srinandhini S., Padmanaban A., Sheeja R.Y., Narayanan V. Synthesis and characterization of MnTe nanoparticles and its photocatalytic activity. *Journal of the Indian Chemical Society*, 2019, **Vol. 46(1)**, p. 147-149.
248. Hu X., Zhang F., Hu Z., He P., Tao L., Zheng Z., Zhao Y., Yang Y., He J. Preparation of 1T′- and 2H–$MoTe_2$ films and investigation of their photoelectric properties and ultrafast photocarrier Dynamics. *Optical Materials*, 2023, **Vol. 136**, 113467. DOI: 10.1016/j.optmat.2023.113467
249. Vikraman D., Hussain S., Jaffery S.H.A., Liu H., Karuppasamy K., Sanmugam A., Jung J., Kim H.-S. Tuning the Layered Thickness of $MoTe_2$ Thin Film for Dye-Sensitized Solar Cells, UV and Visible Spectrum Photodetectors, and Hydrogen Evolution Reaction. *RRL Solar*, 2022, **Vol. 6(12)**, 2200610. DOI: 10.1002/solr.202200610
250. Chandran Y., Arya N., Luhar B., Balakrishnan V. Fabrication of centimeter-scale $MoTe_2$ layers with high chemical stability for hydrogen evolution application. *International Journal of Hydrogen Energy*, 2025, **Vol. 101**, p. 983-989. DOI:10.1016/j.ijhydene.2024.12.477
251. He Y., Boubeche M., Zhou Y., Yan D., Zeng L., Wang X., Yan K., Luo H. Topologically nontrivial 1T'-$MoTe_2$ as highly efficient hydrogen evolution electrocatalyst. *J. Phys. Mater*., 2021, **Vol. 4**, 014001. DOI: 10.1088/2515-7639/abc40c
252. Seok J., Lee J.-H., Bae D., Ji B., Son Y.-W., Lee Y.H., Yang H., Cho S. Hybrid catalyst with monoclinic $MoTe_2$ and platinum for efficient hydrogen evolution. *APL Mater.,* 2019, **Vol. 7**, 071118. DOI: 10.1063/1.5094957
253. Oh J., Park H.J., Bala A., Kim H.-S., Liu N., Choo S., Lee M.H., Kim S.J., Kim S. Nickel telluride vertically aligned thin film by radio-frequency magnetron sputtering for hydrogen evolution reaction. *APL Mater.,* 2020, **Vol. 8**, 121104. DOI: 10.1063/5.0024588
254. Bhat K.S., Barshilia H.C., Nagaraja H.S. Porous nickel telluride nanostructures as bifunctional electrocatalyst towards hydrogen and oxygen evolution reaction. *International Journal of Hydrogen Energy*, 2017, **Vol. 42(39),** p. 24645-24655. DOI:10.1016/j.ijhydene.2017.08.098
255. Garstenauer D., Guggenberger P., Zobač O., Jirsa F., Richter K.W. Active site engineering of intermetallic nanoparticles by the vapour–solid synthesis: carbon black supported nickel tellurides for hydrogen evolution. *Nanoscale*, 2024, **Vol. 16**, p. 20168-20181. DOI: 10.1039/D4NR03397C
256. Elsharkawy S., Kutyła D., Marzec M.M., Zabinski P. Electrodeposition of hydrophobic Ni thin films from different baths under the influence of the magnetic field as electrocatalysts for hydrogen production. *International Journal of Hydrogen Energy*, 2024, **Vol. 61**, p. 873-882. DOI: 10.1016/j.ijhydene.2024.03.045
250. Minegishi T., Ohnishi A., Pihosh Y., Hatagami K., Higashi T., Katayama M., Domen K., Sugiyama M. ZnTe-based photocathode for hydrogen evolution from water under sunlight. *APL Mater.,* 2020, **Vol. 8**, 041101. DOI: 10.1063/5.0002621
258. Jang Y.J., Lee J., Lee J., Lee J.S. Solar Hydrogen Production from Zinc Telluride Photocathode Modified with Carbon and Molybdenum Sulfide. *ACS Appl. Mater. Interfaces*, 2016, **Vol. 8(12),** p. 7748–7755. DOI: 10.1021/acsami.5b07575
259. Junaid M., Batoo K.M., Hussain S.G., Khan W.Q., Hussain S. Photodegradation of CdTe thin film via PVD for water splitting to generate hydrogen energy. *Results in Chemistry*, 2023, **Vol. 6**, 101102. DOI: 10.1016/j.rechem.2023.101102
260. Wang M., Zhou J., Ji J., Song J., Ji W. Performance assessment of solar-driven electrolytic hydrogen production systems enhanced by CdTe PV and sun-tracking device. *Applied Energy*, 2025, **Vol. 390**, 125852. DOI: 10.1016/j.apenergy.2025.125852
261. Veiga L.S., Kumagai H., Sugiyama M., Minegishi T. Efficient hydrogen evolution from water over a thin film photocathode

composed of solid solutions with a composition gradient of ZnTe and CdTe. *Sustainable Energy Fuels*, 2024, **Vol. 8**, p. 2210-2218. DOI: **10.1039/D4SE00067F**

262. Sujita P., Vadivel S., Nasrin Banu G., Neppolian B. Layered -bismuthene maximizes the active sites in Bi_2Te_3 towards electrocatalytic hydrogen evolution reactions. *Journal of Alloys and Compounds*, 2024, **Vol. 1003**, p. 175483. DOI: 10.1016/j.jallcom.2024.175483
263. Yu X., Cao X., Kang W., Chen S., Jiang A., Luo Y., Deng W. Efficient hydrogen production over Bi_2Te_3-modified TiO_2 catalysts: A first principles study. *Surface Science*, 2024, **Vol. 739,** 122401. DOI: 10.1016/j.susc.2023.122401
264. Nath M., De Silva U., Singh H., Perkins M., Liyanage W.P.R., Umapathi S., Chakravarty S., Masud J. Cobalt Telluride: A Highly Efficient Trifunctional Electrocatalyst for Water Splitting and Oxygen Reduction. A*CS Appl. Energy Mater.,* 2021, **Vol. 4(8)**, p. 8158–8174. DOI: 10.1021/acsaem.1c01438
265. Anantharaj S., Kundu S., Noda S. Progress in nickel chalcogenide electrocatalyzed hydrogen evolution reaction. *J. Mater. Chem. A*, 2020, **Vol. 8**, p. 4174-4192. DOI: 10.1039/C9TA14037A
266. Balan A.P., Radhakrishnan S., Neupane R., Yazdi S., Deng L., de los Reyes C.A., Apte A., Puthirath A.B., Manmadha Rao B., Paulose M., Vajtai R., Chu C.-W., Martí A.A., Varghese O.K., Tiwary C.S., Anantharaman M.R., Ajayan P.M. Magnetic Properties and Photocatalytic Applications of 2D Sheets of Nonlayered Manganese Telluride by Liquid Exfoliation. *ACS Appl. Nano Mater.* 2018, **Vol. 11(1),** p. 6427–6434. DOI: 10.1021/acsanm.8b01642
267. Mansoo, S., Tayyab M., Khan M., Akmal Z., Zhou L., Lei J., Anpo M., Zhang J. Recent advancements in Se- and Te-enriched cocatalysts for boosting photocatalytic splitting of water to produce hydrogen. *Res Chem Intermed,* 2023, **Vol. 49**, p. 3723–3745. DOI: 10.1007/s11164-023-05077-5
268. Munonde T.S., Nomngongo P.N. Review on Metal Chalcogenides and Metal Chalcogenide-Based Nanocomposites in Photocatalytic Applications. *Chemistry Africa,* 2023, **Vol. 6**, p. 1127–1143. DOI: 10.1007/s42250-022-00577-0
269. Wang Q., Wang X., Yu Z., Jiang X., Chen J., Tao L., Wang M., Shen Y. Artificial photosynthesis of ethanol using type-II g-C_3N_4/ZnTe heterojunction in photoelectrochemical CO_2 reduction system. *Nano Energy*, 2019, **Vol. 60**, p. 827-835. DOI: 10.1016/j.nanoen.2019.04.037
270. Chen D., Wang A., Buntine M., Jia G. Recent Advances in Zinc-Containing Colloidal Semiconductor Nanocrystals for Optoelectronic and Energy Conversion Applications. *ChemElectroChem*, 2019, **Vol. 6(18)**, p. 4709-4724. DOI: 10.1002/celc.201900838
271. Du M., Li D., Liu S., Yan J. Transition metal phosphides: A wonder catalyst for electrocatalytic hydrogen production. *Chinese Chemical Letters*, 2023, **Vol. 34(9)**, 108156. DOI: 10.1016/j.cclet.2023.108156
272. Ma X., Li W., Ren C., Dong M., Geng, Wang T. Study of iron group transition metal phosphides (M_2P, M = Ni, Co, Fe) for boosting photocatalytic H_2 production. *Separation and Purification Technology*, 2023, **Vol. 316**, 123805. DOI: 10.1016/j.seppur.2023.123805
273. Liu P., Rodriguez J.A. Catalysts for Hydrogen Evolution from the [NiFe] Hydrogenase to the Ni_2P(001) Surface: The Importance of Ensemble Effect. *J. Am. Chem. Soc*. 2005, **Vol. 127(42)**, p. 14871–14878. DOI: 10.1021/ja0540019
274. Cao Sh., Chen Y., Wang C.-J., He P., Fu W.-F. Highly efficient photocatalytic hydrogen evolution by nickel phosphide nanoparticles from aqueous solution. *Chemical Communications*, 2014, **Vol. 50(72),** p. 10427-10429. DOI: 10.1039/c4cc05026f
275. Cao Sh., Wang C.-J., Fu W.-F., Chen Y. Metal Phosphides as Co-Catalysts for Photocatalytic andPhotoelectrocatalytic Water Splitting. *ChemSusChem*, 2017, **Vol. 10(22),** p. 4223-4663. DOI: 10.1002/cssc.201701450

276. Sun M., Liu H., Qu J., Li J. Earth-Rich Transition Metal Phosphide for Energy Conversion and Storage. *Adv Energy Mater.*, 2016, **Vol. 6(13),** 1600087. DOI: 10.1002/aenm.201600087
277. Yang Y., Zhou Ch., Wang W., Xiong W., Zeng G., Huang D., Zhang Ch., Song B., Xue W., Li X. Recent advances in application of transition metal phosphides for photocatalytic hydrogen production. *Chem. Eng. J.*, 2021, **Vol. 405**, 126547. DOI: 10.1016/j.cej.2020.126547
278. Shaheen S., Ali S.A., Mir U.F., Sadiq I., Ahmad T. Recent advances in transition metal phosphide nanocatalysts for H_2 evolution and CO_2 reduction. *Catalysts*, 2023, **Vol. 13(7)**, 1046. DOI: 10.3390/catal13071046
279. Li W., Cao J., Xiong W., Yang Zh., Sun S., Jia M., Xu Z. In-situ growing of metal-organic frameworks on three-dimensional iron network as an efficient adsorbent for antibiotics removal. *Chem. Eng. J.,* 2020, **Vol. 392**, 124844. DOI: 10.1016/j.cej.2020.124844
280. Qi Y., Xu J., Fu Y., Wang Ch., Wang L. Metal-Organic Framework Templated Synthesis ofg-C_3N_4/Fe_2O_3@FeP Composites for Enhanced Hydrogen Production. *ChemCatChem*, 2019, **Vol. 11(15),** p. 3465-3473. DOI: 10.1002/cctc.201900863
281. Zhao Chengxiao, Tang H., Liu W., Han Ch., Yang X., Liu Q., Xu J. Constructing 0D FeP Nanodots/2D g-C_3N_4 Nanosheets Heterojunction for Highly Improved Photocatalytic Hydrogen Evolution. *ChemCatChem*, 2019, **Vol. 11(24)**, p. 6310-6315. DOI: 10.1002/cctc.201901489
282. Zhao S., Xu J., Li Zh., Liu Z., Li Y. Molybdenum disulfide coated nickel-cobalt sulfide with nickel phosphide loading to build hollow core-shell structure for highly efficient photocatalytic hydrogen evolution. *Journal of Colloid and Interface Science*, 2019, **Vol. 555**, p. 689-701. DOI: 10.1016/j.jcis.2019.08.019
283. Wen P., Zhao K., Li H., Li J., Li J., Ma Q., Geyer S.M., Jiang L., Qiu Y. *In situ* decorated Ni_2P nanocrystal co-catalysts on g-C_3N_4 for efficient and stable photocatalytic hydrogen evolution *via* a facile co-heating method. *J. Mater. Chem. A*, 2020, **Vol. 8**, p. 2995-3004. DOI: 10.1039/C9TA08361H
284. Liu Y., Xiang Zh. Fully Conjugated Covalent Organic Polymer with Carbon-Encapsulated Ni_2P for Highly Sustained Photocatalytic H_2 Production from Seawater. *ACS Appl. Mater. Interfaces,* 2019, **Vol. 11(44),** p. 41313–41320. DOI: 10.1021/acsami.9b13540
285. Shen R., Xie J., Ding Y., Liu S., Adamski A., Chen X., Li X. Carbon Nanotube-Supported Cu_3P as High-Efficiency and Low-Cost Cocatalysts for Exceptional Semiconductor-Free Photocatalytic H_2 Evolution. *ACS Sustainable Chem. Eng.*, 2018, **Vol. 7(3),** p. 3243-3250. DOI: 10.1021/acssuschemeng.8b05185
286. Sun Z., Yue Q., Li J., Xu J., Zheng H., Du P. Copper phosphide modified cadmium sulfide nanorods as a novel p–n heterojunction for highly efficient visible-light-driven hydrogen production in water. *J. Mater. Chem. A*, 2015, **Vol. 3**, p. 10243-10247. DOI: 10.1039/C5TA02105G
287. Song Y., Xin X., Guo Sh., Zhang Y., Yang L., Wang B., Li X. One-step MOFs-assisted synthesis of intimate contact MoP-Cu_3P hybrids for photocatalytic water splitting. *Chemical Engineering Journal*, 2020, **Vol. 384**, 123337. DOI: 10.1016/j.cej.2019.123337
288. Yang Z., Xing Z., Feng Q., Jiang H., Zhang J., Xiao Y., Li Z., Chen P., Zhou W. Sandwich-like mesoporous graphite-like carbon nitride (Meso-g-C_3N_4)/WP/Meso-g-C_3N_4 laminated heterojunctions solar-driven photocatalysts. *Journal of Colloid and Interface Science*, 2020, **Vol. 568**, p. 255-263. DOI: 10.1016/j.jcis.2020.02.060